

Water nebulization to counteract urban overheating: Development and experimental test of a smart logic to maximize energy efficiency and outdoor environmental quality

Giulia Ulpiani^{a,*}, Costanzo di Perna^a, Michele Zinzi^b

^a Department of Industrial Engineering and Mathematical Sciences (DIISM), Polytechnic University of Marche, Ancona, Italy

^b ENEA, Via Anguillarese 301, 00123 Rome, Italy

HIGHLIGHTS

- A novel prototype of water nebulizers was optimized to mitigate the urban climate.
- Climate adaptive features were imparted by implementing a fuzzy controller.
- Fuzzy and on-off logics were monitored and compared in two different urban settings.
- The energy saving touched 70% with ambient conditions very close to neutrality.
- The cooling capacity reached -7.5°C mostly dependent on wind.

ARTICLE INFO

Keywords:

Urban climate
Urban heat island mitigation technologies
Evaporative cooling
Water spraying
Smart control
Fuzzy logic

ABSTRACT

Several mature urban climate mitigation technologies have been proposed to date. What mostly hinders their wide implementation is that their efficiency heavily depends on the local microclimatic specificities, since they cannot self-adjust to the environmental changes. This study aims at investigating benefits and impacts of smart logics applied to outdoor cooling, by field testing a web of nebulizers coupled to a bespoke fuzzy controller piloting the pump. The cooling action was tweaked as convenient to maintain comfortable conditions and to avoid energy wastage whenever unneeded. To the best of the authors' knowledge, this is the first application of fuzzy logic to water spraying systems (or to any other controllable urban climate mitigation technology) targeting comfort and energy optimization. The prototype was field monitored in comparison with the conventional on-off control, in two Italian urban contexts (Cfa and Csa climatic zones) over 15 days in the hottest months of the year. The cooling and humidification action was thoroughly characterized by mapping both the horizontal and vertical profiles and by applying advanced Artificial Intelligence techniques to spot the main environmental drivers. The maximum cooling (measured between the sprayed area and an undisturbed reference) touched 7.5°C and 6.14°C in the two locations, respectively. The energy saving achieved under fuzzy control versus the temporized control, was spectacularly high in the wetter and windier location with an average of -51.2% and a maximum of -67.5% . The comfort benefit was also substantial: the temperature never deviated from neutrality by more than $\pm 2^{\circ}\text{C}$, whereas with the on-off, this threshold was surpassed between the 14% and the 20% of the time by even more than 5°C . The results suggest that smartly controlled nebulization is an energy-efficient and comfort-effective strategy to counteract urban overheating. Furthermore, solar-powered solutions are well suited as proved by the preliminary design estimation we included.

1. Introduction

In the Fifth Assessment Report [1], the Intergovernmental Panel on Climate Change advocates, with high confidence, that a warming greater than 1.5°C above pre-industrial levels will be geophysically

unavoidable. *De facto*, 20–40% of the global population already lives in regions where the temperature increment has surpassed this threshold. Besides, human activities heavily impact on the Earth's ecosystems: the envisaged human-induced warming rate is $0.2 \pm 0.1^{\circ}\text{C}$ per decade.

Metropolitan areas are those where the escalation is likely to

* Corresponding author.

E-mail address: g.ulpiani@pm.univpm.it (G. Ulpiani).

Nomenclature	
# _{actual}	Actual quantity (rounded-up)
# _{nominal}	Nominal quantity
A.I.	Artificial Intelligence
AVG	Average Value [°C] or [%]
Counter	Number of pump duty cycles
Cp	Water heat capacity [J/kg °C]
DEV.S	Standard deviation [°C] or [%]
DoD	battery Depth of Discharge [%]
Dt _{avg}	Average mean cooling beneath the spray [°C]
Dt _{max}	Average maximum cooling beneath the spray [°C]
Dt _{min}	Average minimum cooling beneath the spray [°C]
Dt _{neutral}	Temperature difference from neutrality [°C]
E	Daily energy consumption [kWh]
E _{abs/day}	Daily energy absorption [Wh]
E _{module}	Energy per photovoltaic module [Wh]
H	Humidex
HDPE	High Density Polyethylene
Ioh	Horizontal global irradiation [W/m ²]
IQR	Interquartile Range [°C]
ISO	International Organization for Standardization
MAX	Maximum Value [°C] or [%]
MIN	Minimum Value [°C] or [%]
MTSV	Mean Thermal Sensation Vote
NI	National Instruments
P	Cooling Power [kWh/min]
P _{abs}	Total power absorption [W]
P _{actual}	Actual battery power (charged) [Ah]
P _{as}	Partial vapor pressure [hPa]
PE	Cooling Power Index [mcal/cm ² s]
PID	Proportional-Integral-Derivative controller
P _{module}	Power per photovoltaic module [W]
P _{nominal}	Nominal battery power [Ah]
PV	Photovoltaics
Q	Water flow rate [m ³ /min]
RH	Relative Humidity [%]
RTD	Resistance Temperature Detector
t _a	Ambient temperature [°C]
t _{on/day}	Daily operating hours [h]
UHI	Urban Heat Island
UTCI	Universal Thermal Climate Index
ws	Wind Speed [m/s]
η	Efficiency

exacerbate because of urban heat island (UHI) triggers [2]. The ramifications are countless and cut across the fields of energy, comfort, economics and health.

By amalgamating worldwide data (Canada, Israel, Japan, Thailand, United States, ...), the increment in peak electricity demand scatters between 0.45 and 4.6 %/°C with an average premium cost due to UHI effects of 4.6%/°C. The resulting penalty is 21 (± 10.4) We per degree of temperature increase and per person [3]. Besides, air conditioning and hot spells galvanize in a mutually empowering way [4]. Summing up several recent studies on quantitative and qualitative data concerning the penetration of air conditioning around the world, Santamouris [5] concluded that, by 2050, the average cooling energy demand of the residential and commercial buildings will increase up to 750% and 275% respectively. Given the simultaneous increase of urban residents and available income, the increment in cooling energy needs will reach +34% globally, with Indian and Southeast Asian figures about one order of magnitude above the other countries.

Indeed, extensive literature addresses the impact of urban microclimate deterioration on air-conditioning energy consumption (ACEC) as it counts for the 30–50% of the total electric energy consumed during summer in a large part of cities, peaking over 50% in some commercially developed cities [6]. Radhi and Sharples [7] showed a steady ACEC increase as the temperature within urban regions exceeded that in rural areas, with a significant role played by human activities. Li et al.'s study [6] disclosed the vicious loop between urban microclimate deterioration and ACEC augmentation supporting the urge to control certain links in this cycle. Same purpose was pursued via multiple-scenario analysis by Lam et al. too [8], yet focusing on the commercial sector. Toparlar et al. [9] performed 36 energy simulations and reported cooling demand increments up to 90% moving from rural to urban locations, with substantial variance depending on thermal insulation, infiltration rates, presence of greenery aligned with the meteorological wind direction.

Xu et al. [10] addressed the nexus of intense urbanization, building energy and air pollution, concluding that the cooling demand in urban areas was 30% and 17% higher than in the suburban area as for office and residential buildings respectively, with a heating decrement of 23% and 20%. Interestingly, they noticed that the urban heating demand was reduced during polluted days, corresponding to enhanced heat island. In the same vein, Zinzi et al. [11] monitored four Roman areas representative of different urban patterns and building types: UHI was

responsible of a heating consumption reduction up to 21% in residential buildings and 18% in office buildings, while the corresponding cooling consumption increase went up to 74% and 53%. To sum up the existing knowledge, Santamouris computed the magnitude of the cooling load penalty on the basis of a large number of articles, under different climatic and building boundary conditions: for each 1 °C of UHI intensity the cooling load is found to be 20% higher, on average [12].

Against this backdrop, the room for energy savings achievable by cooling the local microclimate in overheated periods makes the imperative for political prioritization much stronger.

Indeed, during heat waves, air-conditioners, refrigerators, and electric fans add a considerable peak demand on electrical utility grids, and on the supply side, high temperatures exert adverse effects on electricity generation, transmission, and distribution, as deeply investigated by Liang et al. for the city of Shanghai [13]. This is a grand social challenge if we consider that by 2050, unprecedented waves of rapid urbanization will drive 70% of global population towards ever-more dense cities [14], interfering with consolidated urban rhythms [15] and fostering the unbridled sprawl of hot spots for extreme environmental issues [16]. Ameliorating the environmental quality and providing equal access to healthier heat-mitigated environments, would thus be a major facilitator for urban metabolism [15].

Several effective solutions are already well characterized and renown, from very simple, long-tradition strategies (greenery [17], water bodies [18], ...) to high-tech, emerging techniques (photovoltaic pavements [19], radiative coolers [20]...).

In an up-to-date comparative study by Santamouris et al. [21] 220 real scale urban projects were analysed in terms of mitigation performance of established technologies (cool roofs, cool pavements, green roofs, urban trees, pools and ponds, sprinklers, fountains, and evaporative towers). Almost 31% of the analysed projects resulted in a peak temperature drop below 1 °C, 62% below 2 °C, 82% below 3 °C and 90% below 4 °C. Water-based technologies exhibited the highest local impact, compared to an equal coverage of greenery, cool materials or solar shadings and especially in the close neighborhood of the cool medium.

Anyway, most of the above technologies typically operate in a passive and non-optimized way which may strongly deteriorate the energy benefit in a year round assessment, contemplating both heating and cooling demand variations. Water bodies, static solar shadings, cool pavements and roofs are effective UHI countermeasures, but, unless

controlled, the temperature reduction occurs over cold days, hot days, summertime and wintertime irrespectively of the actual need for cooling [22]. Furthermore, their seamless operation boosts weathering, ageing and fatigue-driven performance loss [23,24].

Although smart controllers (PID, fuzzy, neural and combos) have been widely investigated for indoor applications (adaptive facades, daylight control, domotics, ventilation ...), the potential for energy conservation outdoors as a potentiation for urban climate mitigation technologies has never been systematically addressed so far. Therefore, no experimentally validated data is available in peer-reviewed literature.

This study was conceptualized to develop and characterize a high-impact mitigation technology, fully optimized in design and control logic so as to bridge this knowledge gap. We focused on the use of water technologies for their high local cooling capacity and among them we selected overhead nebulizers as, compared to sprinklers, fountains or ponds, they process minimum amounts of water to generate a cooling mist that wraps around bystanders and passersby. Besides, water spray acts upon more than a single microclimatic parameter thus being helpful in a variety of contexts: it impacts on both temperature and humidity, it removes dust and enhances air quality, it attenuates solar radiation, including harmful UV, from both direct and indirect sources (against which opaque shadings are ineffective) [25].

Indeed, direct evaporative cooling by water spraying has been extensively used to create pedestrian cool spots in urban locations, notably as more efficient components, stronger constructive methodologies and more adapted management practices came into play. International exhibitions in cities such as Osaka (1970), Seville (1992), Lisbon (1998), Nagoya (2005), and Zaragoza (2008), were valuable stepping stones, as well as some famous projects like Pepsi Pavilion by Fujiko Nakaya, the Tanner Fountain at Harvard University or Le Miroir d'eau in Place de la Bourse (France).

The scientific characterization in terms of microclimatic control proceeded alongside.

Narumi et al. [26] investigated the effect of misting technologies on reducing urban heat fluxes and saving energy. They verified multiple positive impacts, such as lower surface temperatures, limited air-conditioning usage time, improved air-conditioning efficiency. Also, through numerical simulations, they computed cooling demand and urban heat flux reductions over 80% and 60% respectively. Nishimura et al. [27] proposed using novel artificial water facilities to alter the temperature and humidity levels, so as to improve pedestrian comfort. Specifically, they monitored a cool spray hanging over a hot sidewalk in Osaka, running parallel to a pond with water fall and fountain. Field measurements and wind tunnel tests showed reduced temperatures on the leeward side: the degree of temperature decline depended upon the type of device, but especially water spray facilities were effective for cooling (over -6°C against maximum -2°C measured without spraying) and humidification (over +40%). The effect spread out to a distance of nearly 35 m. Again in Osaka, Farnham et al. [28] investigated overhead hydraulic misting nozzles in semi-enclosed spaces and humid climate, where the balance between cooling and undesirable wetting requires careful placement and selection of the nozzles: single-nozzle spraying mists with Sauter mean diameter of 41–45 μm could provide non-wetting or nearly non-wetting cooling with little or no effect on the thermal comfort as verified by effective temperature comparison. Mists of greater diameter were likely to cause wetting even from a height of 25 m. From the thermal perspective, studies by Yoon and Yamada [29] demonstrated, via numerical fluid analysis, that no significant differences in the cooling performance could be imputable to the particles' size, just a longer persistence in a lower position with larger diameters.

Montazeri et al. [30] applied high-resolution Computational Fluid Dynamics based on the 3D unsteady Reynolds-Averaged Navier-Stokes equations to assess the cooling potential of a water spray system (15 hollow-cone nozzles) simulated in a Dutch courtyard under heatwave

conditions (period of July 2006). Validation was based on wind-tunnel measurements and satellite imagery data: the maximum temperature and UTCI reductions were about 7 and 5 $^{\circ}\text{C}$, observed at pedestrian height, with strong thermal stress alleviation up to about 5 m from the spray line.

Despite the longtime application and the numerous simulation-based studies to fully characterize the phenomenon, evaporative cooling has been scarcely investigated in terms of optimized operating mode.

Nunes et al. in Beirut [31] developed a methodology to consider the main influential factors (air temperature, humidity, wind direction, wind speed, water droplet's size, solar radiation and cast shadows). They concluded that "misting systems can be effective in public spaces' microclimatic control of different natures and scales, as long as they are designed for it and in profound connection with many factors such as site's topography, ground surfaces, vegetation, built volumes, and daily and seasonal shade regimes".

This demonstrates how nebulizers' efficiency is strongly site-specific, which is a major drain on successful applications, unless climate-adaptive features are imparted by means of control algorithms.

In the current practice, water nebulizers are generally imposed a continuous operating cycle or, at the utmost, an on-off temporization (with duty cycles of few seconds). The latter solution helps maintaining the relative humidity under a ceiling, usually capped at 65–70% [21].

An exemplary demonstration of controlled nebulization (among the few reported experimentations) comes from Dominguez et al.'s studies [32]: they monitored 128 micro-nebulizers installed in the open areas of the Seville Expo '92, under pergolas (POLIS project). With a flow rate of 0.12 l/min per nozzle, they recorded temperature drops up to 10 $^{\circ}\text{C}$ (when the untreated outdoors stayed at 42 $^{\circ}\text{C}$) and an average of 3–4 $^{\circ}\text{C}$. In spite of the huge cooling, the relative humidity never surpassed 65%: this was achieved by setting the operation to intermittent.

Nonetheless, the optimization of the evaporative process comes from the interplay of a sheer number of parameters (including dry-bulb temperature, vapor pressure, wind-driven dilution, solar-induced secondary phase change, rainfall, ...) which should be somehow included in the decision-making process. Moreover, pumping systems are well suited for fine-grained regulation by either controlling the activation time or modulating the speed with an inverter. Amid the positive impacts:

- the energy expenditure could be cut off anytime convenient, notably when dealing with strong windy conditions and the related unnecessary water losses and dissipation to adjacent spaces.
- The temperature drop could be piloted to stay below the indoor cooling setpoint or to orbit around comfort neutrality. Beyond reducing the operating time of air conditioners [33,34], this would make free cooling and natural ventilation a viable mean for maintaining either outdoor and indoor comfortable conditions. With less anthropogenic heat released by condensing units, the urban ambient temperature could be even 1 $^{\circ}\text{C}$ cooler than in an unmitigated scenario [35].
- Urban resilience would be enhanced: self-adjusting technologies are expected to alleviate the burden of climate change and weather extremes in dense cities and towns, plagued by still low/mid-low adaptation capabilities.
- Potential upgrade to renewable-powered solutions would pave the way to self-sustaining energy systems. Solar-powered aerial misting systems [36] would especially benefit from a control logic that tends to require more power under hotter and sunnier conditions.

To the best of the authors' knowledge, only two conference/symposium papers [37,38] deal with the control of evaporative mist cooling based on outdoor parameters. The authors consider the need to incorporate such variables as control criteria, but in a rigid, unadaptable way: fixed arbitrary thresholds are used to determine whether to start

pumping (e.g. temperature over 28 °C, relative humidity below 70%, wind speed less than 3 m/s, no rainfall in [38]). Moreover, no information is given on the comfort or energy premium of the smart controller compared to a simple temporization. A deeper investigation on the performance control of evaporative cooling is presented in [39], yet it addresses spray passive down-draft systems to cool building indoors with a purely simulation-based approach.

In this study, an innovative rule-based control logic, capable of pondering the pump activation on the concomitant cooling potential was designed, monitored in two different urban settings and compared to alternative solutions so as to quantify the cooling performance, the achieved environmental quality and the energy saving.

Given the amount of variables and the fundamentally chaotic nature of comfort, notably in outdoor spaces, an approximated reasoning, in the form of fuzzy logic, was adopted.

This is the very first time fuzzy control is applied to water spraying systems or to any other controllable UHI countermeasures. Indeed, this work aims at pioneering the introduction of optimized smart controllers into energy systems dedicated to urban climate mitigation, to extend their applicability, enhance urban resilience and rationalize the energy expenditure.

2. Aims, materials and methods

The literature review evidences some limitations and critical aspects related to the investigated technology, in particular:

- no information is available on the potential for energy conservation of an on-off timing that is optimized upon the temporal variations of the local microclimatic conditions;
- no information is available on the potential for tuning the evaporative cooling process to track specific targets (neutral temperature, indoor cooling setpoint, temperature-humidity healthy combinations [40]...);
- no mathematical law has ever been established to link the local cooling to the concomitant environmental variables and spot main drivers and relative weights.
- no information is available on the potential upgrade to renewable-powered solutions.

The experiment was thus structured to solve the above questions and thoroughly investigate the potential of the novel smart prototype we propose, with particular emphasis on the energy and comfort implications. Therefore, we aimed at:

- characterizing the cooling and humidification potential, both in

terms of spatial distribution and of temporal evolution, by linking spread and magnitude to the concomitant climatic context and control action;

- quantifying the energy saving of the fuzzy logic compared to a simple on-off timing in relation to the boundary conditions in different urban settings;
- quantifying the level of achieved thermal comfort, by computing the offset from the neutral temperature, then analyzing its amplitude, its frequency and the repercussions on air humidity;
- determining the main environmental drivers to establish number and typology of sensors needed to feed the fuzzy controller and easily replicate the prototype;
- estimating size and characteristics of self-sustained solutions, by exploiting the link between energy absorption and solar power, *inter alia*.

The following paragraphs introduce methods, tools and materials used in this study to accomplish the above tasks.

2.1. Spraying rack

Nebulization relies on the process of adiabatic saturation. Anyway, if we look at the phenomenon on a psychrometric chart, we would notice that the transformation moves on a quasi-isenthalpic line too: accordingly, in the neighborhood of 30 °C (dry bulb temperature), a temperature drop of 1 °C would raise the relative humidity by 5%. Thus, undue increase of relative humidity has to be carefully governed, as well as potential wetting, not to trigger discomfort events.

Droplet size is a key player. When very fine droplets are blown, the high surface-to-volume ratio guarantees rapid and complete evaporation, maximizing the subtraction of latent heat from the surrounding air [41,42]. Therefore, we selected a set of hollow-cone, micro-nebulizers (or micronizers), with droplet size distribution centred below 10 µm.

A total of 24 nozzles was arranged in a 6x4 horizontal rack symmetrically designed to balance the pressure drops. Each of the 4 branches was fitted with a shut-off valve, to cut off the water supply to the relevant set of nozzles if necessary. The spacing was customizable by simply cutting the polyamide tube into chunks of different lengths. It was set to 1 m after a string of preliminary simulations in ANSYS Fluent [43] as trade-off between magnitude of water coalescence and dilution. Eventually, the spraying rack covered approximately 3mx6m in plan, suspended at about 3 m above the ground. With quick coupling joints the setup was completed within a very short time (less than half a day by a single technician).

The self-compensating 70 bar water pump could supply from 24 to 48 nozzles. The measured electric power absorption was 990 W, while

Table 1
Nebulizing system components.

Item	#	Features	Notes
Water pump	1	Prevalence: 70 Bar Nominal water flow: 31/min Measured water flow (4 × 6 nozzles connected): 1.5 l/min Measured water flow (2 × 6 nozzles connected): 0.72 l/min Measured circuital parameters: 919 W, 228 V, 4.67 A	Accessories: AISI 430 Skinplate carter, manometer, inlet valve, discharge valve, pressure switch for dry run protection
Filter	1	1 × 9" – 3/4" 5 µm melt-blown cartridges	
Tube	1	Polyamide, 1/4" × 50 m long bundle	
Tube clips	50	Steel, 1/4", sealed	
Nozzle	24	0,20 mm cleanable misting nozzle Noxide/S	Steel head with anti-drip check valve
Fitting for nozzle	20	1/4" × 10/24",	
End fitting for nozzle	4	1/4" × 10/24", 90°	
"T" fitting	3	1/4"	
"L" fitting	4		
Shut-off valve	4	on/off slip lock, 1/4", 1150 psi	

the water flow rate, with 24 nozzles in place, was 1.5 l/min. A spring-loaded valve was placed against each orifice to avert dripping under depressurized conditions.

No water storage was in place, because of legionella risk. A melt-down polypropylene microfiber filter was inserted right before the manifold: its dirt-holding capacity prevented any clogging, despite the sensitiveness of nebulizers' geometry. In case of hard water supplied to the system, the insertion of an anti-scale filter was suggested to chemically treat the calcium and magnesium salts and avoid impractical maintenance.

The main components of the evaporative cooling prototype are listed in Table 1.

2.2. Monitored settings

The first monitoring campaign was conducted on the Marche Polytechnic University terrace to gather data over an extensive period (total of 9 days) with no need to set-up and dismantle the monitoring equipment all the times (no transit area nor risk of vandalism).

Each row was secured to a tightened tensioner, running from the overlooking office wall to the mortar wall of the cabin where the pumping and control systems were seated (refer to Fig. 2). A couple of clips were applied to each nozzle fitting to fix its position and orientate the jet direction.

The pump was connected to the local water and electric supply.

The climatic context refers to warm and temperate Cfa conditions according to Köppen and Geiger [44], with significant rainfall all the year round (757 mm on average). Ancona owes its mild climate to strong maritime influences: the average annual temperature is 14.4 °C with a maximum variation of 17.9 °C in summertime and a low of about 5.4 °C in January (monthly average).

The campaign took place in July, which is the warmest (average dry-bulb temperature of 23.3 °C) and the driest month (47 mm of rainfall), and in August 2018. The observation window was set to 10 am–8 pm all the days.

The above experimental setting was customized to the University terrace. Later, the system was replicated in Rome, in a 50 m × 16 m playground in the Centocelle district to double-check the results in a much more complex urban landscape and a different climatic frame: on this occasion, an all-purpose mechanical structure was proposed.

We rigged a very low cost, suspended system (not to occupy public areas) of pulleys, heavy-duty, adjustable straps and tensioned stainless steel cables. The only site prerequisite was the presence of vertical bearing elements on both sides of the spraying rack, such as walls, lampposts, fences, trees, gates and so forth.

The pump was connected to the local water fountain with a T fitting that allowed to provide a seamless supply for both the uses, given the small quota absorbed by the micronizers.

Compared to other Roman municipalities, Centocelle exhibits the highest humidity levels at peak temperature hours, which is worst case scenario for evaporative cooling as it depreciates the partial pressure difference behind state change.

According to the Köppen-Geiger's classification, the local climate features hot-summer Mediterranean characteristics (Cs class) with nuances of temperate continentality.

Significant precipitation is recorded over wintertime, notably in November, with a monthly average of 114 mm against an annual mean of 798 mm.

The driest and hottest month is July with 17 mm of rain and an average temperature of 24.4 °C. Clear, hot days are the norm in August too. Sporadic thunderstorms occur in the afternoon, especially in the northern and eastern neighborhoods of the city (Centocelle included), namely those farther from the sea. In August 2018 (when the monitoring took place), the frequency and severity of night-time squalls were spectacularly high, thus aggravating the humidity conditions in the area (107 mm monthly total recorded by the local meteorological station).

The Roman campaign lasted 6 days. For safety reasons, the equipment was disassembled and re-assembled every day, thus the observed horizon narrowed down to 11 am–7 pm (two hours less than in Ancona).

The ranges of climatic conditions, experienced over the two monitoring runs are displayed in Fig. 1. In Ancona, the average air temperature, humidity and wind speed were 30.7 °C, 59.5% and 2.6 m/s respectively. The corresponding values in Rome were 0.8 °C, 11.6% and 1.8 m/s lower. Also the variability was attenuated in the second location (nearly halved as for air temperature and wind speed) as indicated by the maximum and minimum lines in Fig. 1.

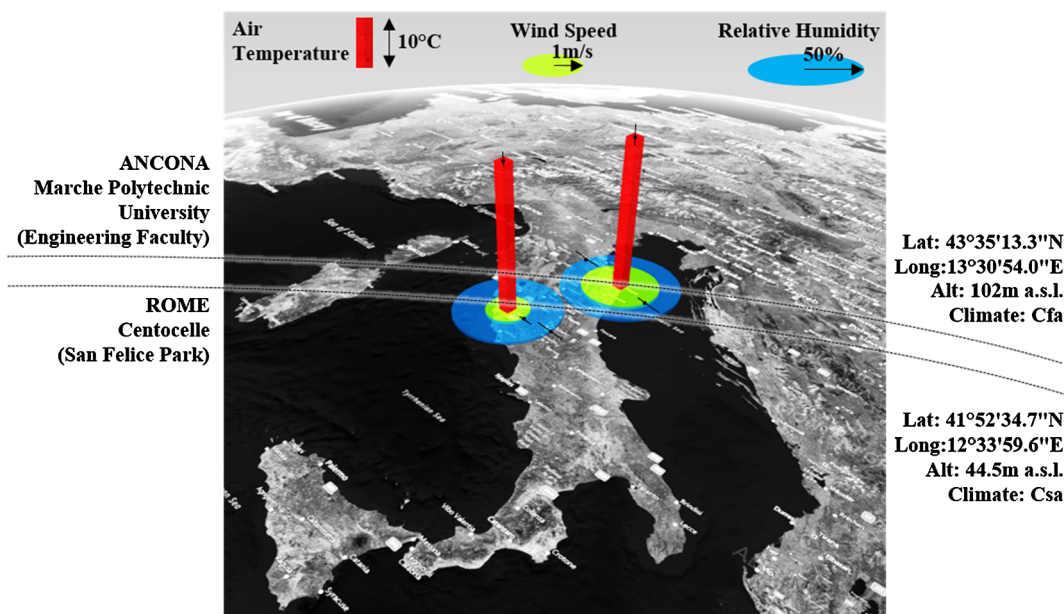


Fig. 1. Geolocalization of the monitoring settings and representation of the mean environmental conditions over the corresponding campaigns. Maximum and minimum lines are additionally displayed.



Fig. 2. Ancona's experimental setup: (1) overview of the terrace and of the nebulizing system; (2) close-up on the office façade, due east; (3) close-up on the cement wall, due west; (4) detail of the thermohygrometers (view from below); (5) detail of the supporting structure on the cement wall; (6) detail of the tightened anchorage on the office façade; (7) detail of the meteorological station, zoomed from the red-bordered region in (1).

2.3. Sensor network

The sensing scheme was platformed in Ancona first. Probes were selected to ensure that all relevant parameters describing the microclimate and the controllers' decisional process were detected with a proper time step.

Accordingly, the following measuring sets were calibrated, installed and connected:

- the weather station, featuring air temperature, relative humidity, solar radiation, wind speed and direction probes. It was placed 50 m away from the spraying system, in un undisturbed, open location and was connected to an LSI Lastem E-Log. The outputs were averaged and saved over a time step of 1 min.
- The thermohygrometric patterner: 5 miniaturized thermohygrometers (PCMINI52 by Michell Instruments) were selected to characterize the cooling and humidification beneath the spray given their high responsiveness (less than 10 s for 90% of the step change) and the in-house provision of a plastic protective cap against wetting. The probes were distributed at the center and mid-points of the ground-projected perimeter of the spraying rack, aligned with the cardinal directions. Such a setup was suggested by the preliminary simulations, that revealed a strong dragging effect exerted by the wind over the atomized droplets: thus, all potential outlets had to be monitored to make sure the cone of action was intercepted. A white

screen prevented solar-induced bias. The height was set to 1.1 m which is the center of gravity for a standing person according to ISO 7726 [45]. This sensing subset was connected to a National Instrument acquisition module NI 9205 for voltage inputs. The acquisition was set to 100 samples at 1 kHz.

The technical specifications of all the above probes are detailed in Table 2, along with a schematization of the reciprocal positioning (3D models of the monitored settings and CAD of the nebulized areas).

Additionally, a rain detector (Kemo M152) was incorporated to avoid spraying under the rainfall. It was connected to a universal acquisition module (NI 9219) set to acquire 10 samples at 1.95 Hz.

All data were transmitted to a dedicated laptop via Ethernet connection.

In addition to the above sensors, a mechanic flowmeter and a manometer were connected to the pump line. They were used to preliminarily check the pump operative conditions and sporadically verify their potential variations. Manometer measurements demonstrated that no pressure drops significantly affected the efficiency of water nebulization. Indeed, the use of constant pressure pumps is recommended to avert the adverse impacts of dirt, limestone, dust, corrosion agents that might occlude the orifices and alter the cooling performance: as a consequence, whatever the water flow running through the hydraulic circuit, the 70 bar pressure was maintained.

The activation of the pump was governed by a digital Input/Output

Table 2

Sensor network: specifications and schematic view of the relative positioning.

Measure	Sensor type	Position	Range	Accuracy	Responsiveness
<i>Weather station</i>					
Air temp. + Relative humidity	Thermo hygrometer	Undisturbed h = 1.7 m	-30 °C ÷ 70 °C 0 ÷ 100%	0.2 °C 1.5% (5 ÷ 95%, 23 °C) 2% (< 5, > 95%, 23 °C)	T (90%) = 10 s
Wind velocity and direction	Cup anemometer	Undisturbed h = 2.0 m	0 ÷ 60 m/s 0 ÷ 360°	1.5% 1°	$\tau(63\%) = 2.5 \text{ s}$ $\tau(63\%) = 0.7 \text{ s}$
Solar radiation	Radiometer	Undisturbed h = 1.5 m	0-2000 W/m ²	< 5%	T (90%) < 30 s
<i>Thermohygrometric patterner</i>					
Air temp. + Relative humidity	Mini thermo hygrometer	Centre and mid projected perimeters h = 1.1 m	-20 °C ÷ 80 °C 0 ÷ 100%	± 0.2 °C ± 2% (10–90%)	T (90%) < 10 s

ANCONA MONITORING SETTING

Meteorological Station
Thermohygrometer

Nebulized Area

University Building

47m

Nebulized Area

- Dimensions in meters -

VERTICAL VIEW

2.5 3.3
2.1 1.7

Nozzle
Thermohygrometer
Thermohygrometer (Rome only)

ROME MONITORING SETTING

Church
Church Square
Nebulized Area
95m
16m

PLAN VIEW

1.25 1.85
1 0.5

module (NI 9401), directly connected to the solenoid valve.

Finally, the water temperature at the nozzle outlet was characterized in its daily swings, by performing spot measurements with an RTD - Pt100. Over the first monitoring campaign, this parameter changed from a minimum of 13 °C to a maximum over 30 °C, while in Rome it stayed within the 19 ± 1 °C range. That was the combined effect of high pressure pumping and heat transmission along the hydraulic circuit. Additionally, both piping and nozzle headers were heated up by the sun. Despite this, as substantiated by several previous studies [41,46,47], even relatively large droplets (hundreds of microns) tend to annul their relative velocity with air and to cool down to the wet bulb

temperature within a meter of the injection. In case of micron-sized particles of about 10 µm this space narrows down to approximately 8 mm [41]. This implies that the net cooling loss due to sensible heat transfer was negligible and any counter effect from hot supply remained confined to the very close neighborhood of the nozzle.

In Rome, the meteorological station was located 16 m away from the spraying system, at the northern edge of the park's protected perimeter. It was aligned with the three Michell sensors along the north-south axis. In doing so, we ensured equal solar shading since a parallel line of trees provided shadow to the three probes from approximately 4 pm on.

On the 27th of August, after three days of continuous nebulization to check test the system and right before starting the investigation on the control logics, five additional temperature and humidity probes were installed to further characterize the phenomenon. The temperature reading was accurate to 0.3 °C, while that of relative humidity to ± 2%. The probes (ATMOS 14) were plugged into two dataloggers DECAGON EM60Gs, notably:

- a cluster of four sensors was assembled on a tripod placed in the middle of the mist (refer to the CAD in Table 2) at 1.1 m, 1.7 m, 2.1 m e 2.5 m above the ground; in this way both the horizontal and the vertical thermohygrometric profiles were retrieved simultaneously;
- a detector was placed about 100 m away from the nebulizers, mounted at about 2.5 m above the ground in the church square as a reference for a totally undisturbed (no evaporation from water nor evapotranspiration from greenery), open (windy and sunlit) location.

Other than that, the sensor network was the same as in Ancona.

Either location, the sampling rate was set to 10 s to guarantee enough responsiveness to the rapidly changing conditions beneath the

spray and process the control action on the pump accordingly. All records were averaged and databased with a 1-minute time step (loop time) to smooth spikes and misreadings.

The experimental setups are pictured in Figs. 2 and 3.

2.4. Controller

Approximate reasoning (in the form of fuzzy logic) is widely renowned to be a successful control strategy anytime objective and subjective spheres conflate, as when it comes to microclimatic comfort [48,49].

The theoretical basis was laid by Zadeh in the 1960s [50] to expand the crisp-set approach into continuous classification. Fuzzification loosens the Boolean way of assigning elements to the corresponding set (non-membership equal to 0 and full membership equal to 1) by contemplating all the intermediate grades of belonging in the shape of membership functions: elements can thus partly befit more than a single set.

Through a metric of linguistic variables, linguistic terms and membership functions, crisp data is reshaped to become manageable via a finite set of logical rules. Such intuitive, mathematical-model-free approach is a time saving asset that outperforms conventional PID or on/off controllers in case of chaotic/nonlinear time-variant working



Fig. 3. Rome's experimental setup: (1) overview of the park and of the nebulizing system; (2) detail of the pulley system on the cable tightened between the trees, due east (3) close-up on the tree straps (4) detail of the return pulleys on the fence, due west; (5) detail of the meteorological station; (6) detail of the tripod for the vertical thermohygrometric mapping; (7) detail of the probe mounted on a tree in the church square (the nebulizing system is red-bordered). (For interpretation of the references to colour in this figure legend, the reader is referred to the web version of this article.)

conditions [51–53] as it can embrace a virtually limitless number of parameters in the decision-making process. Besides, heuristics and past experience can be integrated into the control system, mimicking human reasoning [54].

In this context, a major challenge was to indoctrinate the controller with the right set of input parameters.

Beyond temperature, other three environmental variables were contemplated to size the call for nebulization: (a) humidity, as it controls the evaporative processes (of water droplets as well as from human skin), (b) wind, that reinforces convective heat dissipation and dilutes the water mist thus increasing the evaporation rate, until transport phenomena overtake, (c) solar radiation, that represents the main heat gain. Consequently, direct indices or indices based on linear equations, where the above parameters are lumped together and appropriately weighted [55], were used to drive the control action, namely:

- offset from the neutral air temperature (Dt_{neutral}) computed on the minimum temperature recorded beneath the spray. This was the major driver. The neutral temperature was set to 27.2 °C, according to an up-to-date study performed in Rome [56]: it was obtained via a transversal field survey and a linear regression analysis between Mean Thermal Sensation Votes (MTSVs) and air temperature in summertime. Not to make it a strict target (which was unlikely to be the case given the room for acclimatization and thermal tolerance in outdoor spaces [57]), a series of symmetric acceptability ranges was defined around neutrality and used to weight the control action.
- Solar radiation. This parameter was introduced as a precautionary measure to arbitrate borderline cases of incipient overheating at peak hours.
- Humidex (H). This linear index correlates air temperature t_a [°C] and relative humidity RH [%] according to the following equations [58]:

$$H = t_a + \frac{5}{9}(p_{as} - 10) \quad (1)$$

$$p_{as} = 6.112 * \left(10^{\frac{7.5+t_a}{237.7+t_a}} \right) \frac{RH}{100} \quad (2)$$

where p_{as} is the vapour pressure in hPa. Humidex was validated in outdoor environments and was first formulated for weather forecast to support people coping with summer thermal strain [59,60]. It is recognized by the European Commission [61] and is becoming established in America too [62].

- Cooling power index (PE): it conveys the combined effect of temperature and wind speed on human comfort by quantifying the cooling of the human body in $\text{mcal}/(\text{cm}^2\text{s})$. It was proposed by Vinje in the following form [63]:

$$PE = 20.52ws^{0.42}(36.5 - t_a) \quad (3)$$

where ws is the wind speed in meters per second. PE is a suitable climate indicator for cities [64] that has gained an increasing acceptance in representing summer comfort conditions. It was used in Greece to map the distribution of comfort conditions for energy purposes and in presence of passive or hybrid cooling systems [65,66], by Gómez et al. [67,68] to characterize the thermal comfort in the cityscape with attention to the green areas (evapotranspiration) and by Ghani et al. [69] to assess thermal comfort in an outdoor air-conditioned area in a hot and arid environment.

The H and PE scales of comfort are reported in Table 3. Apparently, such indices are well suited for fuzzification as they already come in the form of linguistic variables and sub-ranges.

A second challenge behind the setup of the fuzzy controller was the definition of the rule set (300 if-then clauses in total). It was tuned according to the following criteria:

- in the closest neighborhood of the neutral temperature, the spraying was activated just in case of simultaneous occurrence of sunny (global solar radiation above 350–400 W/m²), stagnant (PE < 5) and dry (H between 20 and 29) conditions;
- in case of cooling power index within the cool/cold degree of comfort and simultaneous acceptably comfortable Humidex values, the pump was switched off as this combination entailed low temperatures;
- when PE stayed above 11 and H was above 30, either the temperature was low or the wind speed was high with considerable moisture content in the air. Accordingly, the spraying was negated;
- when PE lied in the hot/mild subranges and H was in the comfortable subrange the pump went on since the air was expected to be hot and dry;
- in case both PE and H reached high values, the air temperature was uncomfortably high and the spray was activated.

The controller was platformed in LabVIEW [70]. The settings are detailed in Appendix, together with the membership functions charts.

Whatever the case, the fuzzy logic was enabled above a given threshold temperature, set to 26 °C. Such value corresponds to the indoor summer setpoint: it means that until it was surpassed, the outdoors was fresher than the ideally comfortable indoors.

A second constraint was obviously given by the presence of the rain: any time the rain detector sent a positive voltage signal, the whole spray routine was bypassed.

As a comparative benchmark, an on-off control was implemented in the same Virtual Instrument (VI). Following the manufacturer's instructions, the duty cycle was of few seconds, namely 20 s activation and 10 s poweroff.

2.5. Post processing methodology

Four main aspects were investigated: cooling, humidification, energy and comfort. The first two denote the performance of the proposed technology as a climatic mitigator. Indeed, both temperature and relative humidity define when climatic conditions become unpleasant or even deadly, consistently with human thermal physiology: heat accumulation occurs when the outdoors exceeds the body core temperature (second law of thermodynamics) or when the sweat rate can no longer compensate [71]. Water nebulization impacts upon both aspects.

The temperature and humidity distribution, patterned by the 5 thermohygrometers, was analyzed both in time (temporal gradient) and space (difference from the unmitigated location) on a daily basis, in the following way:

- the minimum temperature recorded under the spray was compared to the temperature in the undisturbed locations. The statistical distribution of the daily differences was computed (percentiles and inter-quartile range) together with the absolute maximum, minimum, the average and the standard deviation, over both the whole observation windows (10 am–8 pm in Ancona, 11 am–7 pm in Rome) and the time of actual nebulization. This was to verify

Table 3
Comfort thresholds in terms of humidex and cooling power index.

H range	Degree of comfort	PE range [mcal/(cm ² s)]	Degree of comfort
< 29	Little or no discomfort	< 5	Hot
30 ÷ 34	Noticeable discomfort	5 ÷ 10	Mild
35 ÷ 39	Evident discomfort	11 ÷ 15	Cool
40 ÷ 45	Intense discomfort (avoid exertion)	16 ÷ 22	Cold
> 45	Dangerous discomfort	23 ÷ 30	Very cold
> 54	Heat stroke probable	> 30	Extreme cold

- whether the highest temperature drop occurred during the spraying or with a certain delay, due to secondary evaporation and inertial effects. Additionally, the cooling peak was related to the time of the day to look for statistical patterns for each control logic.
- The temperature and humidity variation recorded by each probe was calculated at every time step and the location (center, north, south, west, east) of the maximum was pinpointed. Therefore, the frequency distribution of the most responsive zones was derived. The degree of skewness was interpreted in terms of local turbulence and boundary effects. The absolute maximum of temperature decrement and of humidity increment was then associated to both the relevant sensor and the spraying duration (computed as the antecedent total time of continuous spraying) to strike causal links between time, location and aggregated water flow.
 - The role of the environmental variables was investigated by means of evolutionary algorithms. This is crucial in terms of urban planning to define selection criteria for the installation sites. Special care was devoted to wind patterns as they strongly affect the evaporative cooling efficacy of overhead nebulization systems. This is the first time that such an analysis is carried out on the basis of experimental data.

To determine the consumption rate and compute the energy saving achieved by the fuzzy logic, a counter was incorporated in the VI: it kept track of the number of 10 s-lasting duty cycles over which the pump was activated within the 1-minute window ($0 \leq \text{Counter} \leq 6$).

Therefore, the water flow rate and power consumption were calculated as follows:

$$P [\text{kWh}/\text{min}] = 0.919 \cdot \text{Counter} \cdot 10/3600 \quad (4)$$

$$Q [\text{m}^3/\text{min}] = 0.0015/6 \cdot \text{Counter} \quad (5)$$

Indeed, from the energy perspective, the mainstay of a rule-based, heuristic approach against a conventional on-off timing is that spray duration becomes the tuning dial to either strengthen or soften the cooling capacity to make sure that no more than enough water and electricity is consumed to preserve comfortable conditions.

The cooling was thus administered according to an adjustable protocol. The elementary dosage was that of a 10 s lasting supply (duty cycle duration) with a water flow of 1.5 kg/min. Assuming the latent heat of vaporization equal to 2437 kJ/kg at 27.2 °C (neutrality), the resulting elementary energy package was:

$$E_{\min} = 2437 \text{ kJ/kg} \cdot \frac{1.5 \text{ kg/min}}{60 \text{ s/min}} \cdot 10\text{s} = 609 \text{ kJ} \quad (6)$$

Table 4
General information on the two monitoring runs.

DATE	CONTROL	ta [°C]	RH [%]	ws [m/s]	Ioh [W/m²]	E [kWh]	Q [m³]	Dt _{max} [°C]	Dt _{min} [°C]	Dt _{avg} [°C]
FIRST MONITORING CAMPAIGN (ANCONA)										
13/07/2018 ON-OFF		30.3	55.2	2.1	710.9	6.13	0.60	2.81	0.18	1.46
14/07/2018 ON-OFF		33.3	54.2	2.6	696.9	6.13	0.60	3.24	0.17	1.55
15/07/2018 ON-OFF		30.9	64.5	2.2	645.3	6.13	0.60	3.13	0.87	1.84
13/08/2018 FUZZY		32.6	57.4	2.8	619.1	4.60	0.45	2.74	0.05	1.33
15/08/2018 FUZZY		29.0	59.9	2.9	525.3	1.99	0.19	2.18	0.95	1.52
16/08/2018 FUZZY		30.0	50.8	2.2	633.0	3.11	0.30	2.29	0.38	1.36
17/08/2018 FUZZY		29.8	57.9	2.5	632.2	2.37	0.23	2.32	0.27	1.35
18/08/2018 FUZZY		29.9	66.8	2.5	621.2	2.52	0.25	2.51	0.97	1.81
19/08/2018 FUZZY		30.2	68.7	3.3	596.8	3.35	0.33	2.57	1.36	2.01
SECOND MONITORING CAMPAIGN (ROME)										
24/08/2018 NO STOP		31.9	44.2	0.7	502.8	7.35	0.72	2.37	-0.77	0.70
25/08/2018 NO STOP		29.3	58.0	1.2	467.0	7.35	0.72	1.89	-0.20	0.92
27/08/2018 NO STOP		28.0	38.1	0.9	572.1	7.35	0.72	2.30	-0.86	0.85
28/08/2018 ON-OFF		29.6	45.9	0.7	561.9	4.90	0.48	1.76	-1.90	-0.06
29/08/2018 FUZZY		30.5	49.0	0.7	489.4	3.80	0.37	1.59	-0.67	0.43
30/08/2018 FUZZY		30.1	52.2	0.7	539.7	3.65	0.36	1.25	-0.95	0.18

The fuzzy controller supplied as much 609 kJ packages as necessary to track the comfort zone.

Conversely, the on-off supplied double the fuzzy elementary package, twice in a minute time, irrespective of the actual call for cooling and over all the time slot of activation.

Beyond either under and overcooling risks, such an untargeted control tends to consume much more energy than necessary, undercutting the potential for renewables-fuelled solutions.

In this work, given that the fuzzy incorporated solar radiation in the decision making process boosting the system only under hot, sunny conditions, we proposed PV-powered high pressure water misting technology as the most promising self-sustaining arrangement. We estimated the photovoltaic requirements and, ultimately, delineated possible design provisions.

The comfort assessment was based on the offset from thermal neutrality (magnitude and frequency distribution). By perusing the input and output parameters used to drive the control, we could spot on which occasions the on-off penalty was emphasized.

Finally, direct comparison between the on-off and fuzzy controllers (on all the four investigated aspects) was performed over days of comparable (almost equal) weather conditions, to provide meaningful ground for confrontation.

3. Results

In the following paragraphs, all the major findings and observations are discussed.

Table 4 was used to spot the representative days for direct comparison between the logics: air temperature, relative humidity, wind speed and horizontal irradiation (averaged over the time slots of spray activation) were daily averaged together with the total electric and hydric consumption and the maximum, minimum and average cooling beneath the spray. The selected days are highlighted by a solid red border and a dashed blue border as for the on-off and fuzzy logic respectively, over the two monitoring runs.

3.1. Cooling and humidification

In Ancona (**Table 5**), the maximum cooling under fuzzy control was 7.4 °C and was recorded around 11:40am on the 13th of August. The 99th percentile was close to 7 °C. It is no coincidence that the air temperature on that day was the highest recorded, with a daily mean of 32.6 °C. In fact, higher dry-bulb temperature at equal specific humidity, implies greater capacity to accommodate extra water vapor per kg of

Table 5
Daily cooling statistics recorded during the first monitoring campaign.

DAY	LOGIC	COOLING	Percentiles				IQR	MAX	When?	MIN	AVG	DEV.S
			99°	90°	50°	1°						
13 Jul 2018	ON-OFF	Dt_max under spray	4.84	4.35	2.79	0.31	1.45	4.90	11:49	0.18	2.81	1.05
		Dt_min under spray	1.77	1.47	0.81	-3.54	1.88	1.92	13:57	-4.19	0.19	1.47
		Dt_avg under spray	2.45	2.18	1.78	-0.71	0.89	2.55	13:57	-0.78	1.46	0.82
14 Jul 2018	ON-OFF	Dt_max under spray	7.22	5.46	2.92	0.07	1.87	7.49	11:22	-0.01	3.24	1.57
		Dt_min under spray	1.74	1.24	0.43	-2.28	1.52	1.95	12:47	-2.83	0.17	1.01
		Dt_avg under spray	3.10	2.28	1.70	-0.37	0.67	3.24	11:35	-0.43	1.55	0.76
15 Jul 2018	ON-OFF	Dt_max under spray	5.66	5.04	3.15	0.32	1.91	6.05	11:46	0.26	3.13	1.47
		Dt_min under spray	2.19	1.95	1.26	-1.75	1.73	2.48	11:25	-2.17	0.87	1.00
		Dt_avg under spray	3.40	2.89	2.09	-0.01	1.13	3.60	11:25	-0.18	1.84	0.94
13 Aug 2018	FUZZY	Dt_max 10am-8pm	6.81	5.04	2.76	0.02	1.98	7.39	11:38	-0.20	2.74	1.64
		Dt_min under spray	6.86	5.09	2.94	0.27	1.83	7.39	11:38	0.03	3.10	1.40
		Dt_avg 10am-8pm	1.47	1.20	0.55	-4.15	1.47	1.54	15:32	-4.37	0.05	1.29
13 Aug 2018	FUZZY	Dt_min under spray	1.47	1.23	0.79	-4.01	1.34	1.54	15:32	-4.24	0.24	1.23
		Dt_avg 10am-8pm	2.71	2.35	1.63	-0.40	1.60	2.91	11:38	-0.85	1.33	0.93
		Dt_avg under spray	2.74	2.38	1.81	-0.31	0.90	2.91	11:38	-0.40	1.57	0.78
15 Aug 2018	FUZZY	Dt_max 10am-8pm	4.62	3.37	2.41	-0.08	1.35	5.08	11:22	-0.34	2.18	1.15
		Dt_min under spray	3.51	3.02	2.46	1.33	0.53	3.59	16:24	0.47	2.44	0.48
		Dt_avg 10am-8pm	2.96	2.46	1.10	-1.31	1.13	3.04	11:55	-1.62	0.95	1.05
16 Aug 2018	FUZZY	Dt_min under spray	1.54	1.40	1.17	-0.48	0.29	1.61	13:06	-1.43	1.12	0.34
		Dt_avg 10am-8pm	3.50	2.81	1.67	-0.29	0.88	3.68	11:22	-0.54	1.52	0.97
		Dt_avg under spray	2.20	2.03	1.75	0.59	0.30	2.27	13:45	0.08	1.72	0.30
16 Aug 2018	FUZZY	Dt_max 10am-8pm	4.27	3.90	2.52	-0.22	1.57	4.45	11:51	-0.31	2.29	1.23
		Dt_min under spray	4.20	3.44	2.59	1.48	0.43	4.38	16:52	1.20	2.66	0.59
		Dt_avg 10am-8pm	1.45	1.32	0.86	-1.83	1.53	1.56	13:11	-2.18	0.38	1.01
16 Aug 2018	FUZZY	Dt_min under spray	1.49	1.36	1.19	-1.53	0.33	1.56	13:11	-1.79	0.88	0.77
		Dt_avg 10am-8pm	2.35	2.12	1.76	-0.37	1.17	2.57	13:33	-0.58	1.36	0.83
		Dt_avg under spray	2.45	2.14	1.88	0.78	0.30	2.57	13:33	0.61	1.80	0.37
17 Aug 2018	FUZZY	Dt_max 10am-8pm	4.50	3.86	2.63	-0.17	1.66	4.73	11:37	-0.29	2.32	1.24
		Dt_min under spray	4.25	3.58	2.74	0.87	0.45	4.54	11:41	0.65	2.74	0.62
		Dt_avg 10am-8pm	1.83	1.65	1.10	-3.44	2.29	1.95	12:05	-3.97	0.27	1.51
17 Aug 2018	FUZZY	Dt_min under spray	1.82	1.70	1.42	-3.23	0.38	1.95	12:05	-3.67	1.03	1.12
		Dt_avg 10am-8pm	2.62	2.39	1.80	-0.78	1.48	2.94	12:05	-0.95	1.35	1.07
		Dt_avg under spray	2.60	2.41	2.08	-0.60	0.49	2.94	12:05	-0.78	1.91	0.67
18 Aug 2018	FUZZY	Dt_max 10am-8pm	5.23	3.63	2.79	0.25	1.29	5.42	11:55	0.05	2.51	1.21
		Dt_min under spray	5.21	3.43	2.98	1.33	0.35	5.42	11:55	0.39	3.04	0.58
		Dt_avg 10am-8pm	2.41	2.05	1.56	-2.00	1.87	2.53	11:37	-2.13	0.97	1.16
18 Aug 2018	FUZZY	Dt_min under spray	2.35	2.06	1.85	-0.34	0.26	2.39	11:55	-1.47	1.80	0.41
		Dt_avg 10am-8pm	3.35	2.81	2.22	-0.08	1.30	3.50	11:37	-0.29	1.81	0.99
		Dt_avg under spray	3.33	2.78	2.52	0.37	0.28	3.43	11:55	0.29	2.48	0.39
19 Aug 2018	FUZZY	Dt_max 10am-8pm	5.10	3.98	2.80	0.20	1.25	5.35	11:56	0.12	2.57	1.23
		Dt_min under spray	5.15	3.86	2.97	1.29	0.72	5.35	11:56	0.89	3.06	0.69
		Dt_avg 10am-8pm	3.13	2.64	1.47	-0.73	1.18	3.46	11:56	-1.05	1.36	1.00
19 Aug 2018	FUZZY	Dt_min under spray	3.16	2.64	1.66	-0.07	0.82	3.46	11:56	-0.53	1.72	0.64
		Dt_avg 10am-8pm	3.77	3.28	2.22	0.07	1.32	4.14	11:56	-0.10	2.01	1.07
		Dt_avg under spray	3.88	3.25	2.46	0.65	0.88	4.14	11:56	0.24	2.42	0.65

▀ █ ≥80% full/scale ▀ █ ≥60% full/scale ▀ █ ≥40% full/scale ▀ █ ≥20% full/scale ▀ █ <20% full/scale

dry air and, ultimately, higher evaporation rates: as the phase change accelerates and persistence time decreases, a larger number of droplets partake in the evaporative cooling within a smaller neighborhood of the injections which explains the magnitude of the local temperature drop. This is further demonstrated if we look at the time lag between the 99th percentile computed over the whole observation window (10 am–8 pm) and that over the intervals of actual activation (Counter > 0). Only

over hot days no delay occurred between maximum temperature drop and poweroff, meaning that the evaporation was facilitated and speeded up.

By contrast, on the coldest observed day (15th of August, 29 °C on average), the cooling peaked at about 5 °C, with the highest values (99th percentile) usually reached after the pump was switched off. Under fuzzy logic operation, this was a combined effect of reduced

potential for humidification and reduced need for cooling.

Yet, as the temperature dependency is a property of the phenomenon rather than of the controller, the same occurred under on-off operation. On the 14th of July, when the temperature was 33.3 °C on average (0.7 °C higher than the hottest day in the fuzzy observation period) the maximum temperature drop reached 7.5 °C, again around 11:30am, with 1% of the readings over 7.2 °C. Conversely, on the coldest day (13th of July, 30.3 °C on average) the peak decremented to less than 5 °C. On those days, all the other environmental variables were almost equal on average (difference of about 2% in relative humidity, of 0.5 m/s in wind speed, of 14 W/m² in solar radiation); therefore, a rise of about 3 °C was responsible of a 50% increment of the cooling capacity.

Also, the interquartile range was affected. Hot days were the only ones over which the IQR computed on the maxima outweighed that on the minima, with both hitting their high. This entails that the spread around the values of temperature drop was much more pronounced and, ultimately, that the comfort conditions beneath the spray were strongly diversified in time.

In Rome (Table 6), most of the above considerations were confirmed, although the boundary conditions were substantially different because of: (1) the combination with the evapotranspiration processes and the solar shading from the local greenery; (2) the very low wind speed due to the orientation of the urban canyon, counter to the prevailing winds.

With the 16 m-distant meteorological station used as reference for the calculation, the maximum temperature drop under fuzzy operation ranged between 3.3 and 4.4 °C, recorded right after the morning

activation (11:00 am) or over peak hours (around 2 pm).

By looking at the 99th percentile (4.2 °C on the 29th of August and 3 °C the day after), it appears that the maximum cooling was simultaneous to the water emission: no delay was recorded, thus most of the highest temperature drops occurred while the system was running.

Again the highest impact was achieved on the hottest day.

Under on-off operation the cooling was more intense, with a maximum of 6.1 °C detected at 2:21 pm, 1% of the readings above 5.5 °C and 10% over approximately 4 °C. The average stayed about 0.15 °C above that of the fuzzy control, while the IQR was significantly narrower.

This happened because the fuzzy algorithm aimed at comfort preservation, not at the maximum achievable cooling: it switched off the pump around 5 pm, while, the on-off controller continued to power the nebulizers until 7 pm, when not just the air was slightly fresh, but the sun was shaded and the water was colder (less heat gains along the pipeline). The temperature was lowered down to approximately 25 °C causing discomfort and unnecessary energy and water consumption.

Interestingly, continuous and temporized operations showed very similar cooling capacity. In the first three days of monitoring campaign, when the system was checked, the pump was left on over the whole day. The maximum temperature reduction was 6.2 °C (basically equal to that recorded with the on-off control right the day after) with 99% of the readings below 5.3 °C. On the other side, significant drops occurred much more frequently with an average of –2.3 °C and 10% of the readings over –4.4 °C.

In terms of humidification, the location played a pivotal role. In Ancona (where the relative humidity was more than 10% greater than

Table 6

Daily cooling statistics recorded during the second monitoring campaign. Refer to Table 5 as for the icons meaning.

DAY	LOGIC	COOLING	Percentiles				IQR	MAX	When?	MIN	AVG	DEV.S
			99°	90°	50°	1°						
24/08/18	NO STOP	Dt_max 11am-7pm	4.77	3.96	2.02	1.08	1.01	5.27	13:55	0.73	2.37	0.92
		Dt_min 11am-7pm	1.26	0.34	-0.73	-2.82	1.17	1.41	13:48	-3.34	-0.77	0.90
		Dt_avg 11am-7pm	2.32	1.76	0.59	-0.80	1.09	2.60	13:55	-1.02	0.70	0.74
25/08/18	NO STOP	Dt_max 11am-7pm	4.18	3.55	1.68	0.21	2.32	4.52	14:00	0.12	1.89	1.22
		Dt_min 11am-7pm	1.83	1.39	-0.24	-2.43	2.16	2.02	14:00	-2.77	-0.20	1.17
		Dt_avg 11am-7pm	2.81	2.22	0.89	-0.43	1.89	3.06	14:00	-0.68	0.92	0.99
27/08/18	NO STOP	Dt_max 11am-7pm	5.34	4.36	1.93	0.94	0.87	6.15	14:00	0.72	2.30	1.10
		Dt_min 11am-7pm	1.14	0.56	-0.76	-3.85	1.59	1.28	18:48	-4.08	-0.86	1.16
		Dt_avg 11am-7pm	1.97	1.59	0.96	-1.03	0.82	2.19	14:24	-1.23	0.85	0.64
28/08/18	ON-OFF	Dt_max 11am-7pm	5.54	3.95	1.44	0.38	0.93	6.14	14:21	0.31	1.76	1.21
		Dt_min 11am-7pm	0.35	-0.66	-1.50	-6.03	1.60	0.68	11:00	-6.56	-1.90	1.30
		Dt_avg 11am-7pm	1.39	0.81	-0.03	-2.10	0.75	1.57	14:21	-2.26	-0.06	0.69
29/08/18	FUZZY	Dt_max 11am-7pm under spray	4.22	3.14	1.52	-0.06	1.46	4.36	13:58	-0.14	1.59	1.03
		Dt_min 11am-7pm under spray	4.26	3.37	1.82	0.41	1.14	4.36	13:58	0.31	2.06	0.88
		Dt_avg 11am-7pm under spray	1.85	0.13	-0.58	-2.66	0.85	1.11	13:50	-2.89	-0.67	0.71
30/08/18	FUZZY	Dt_max 11am-7pm under spray	0.91	0.26	-0.79	-2.76	1.10	1.11	13:50	-2.89	-0.78	0.82
		Dt_avg 11am-7pm under spray	1.95	1.30	0.33	-1.18	0.87	2.29	13:50	-1.47	0.43	0.64
		Dt_max 11am-7pm under spray	1.99	1.48	0.54	-1.24	0.92	2.29	13:50	-1.47	0.60	0.70
		Dt_max 11am-7pm under spray	3.02	2.48	1.44	-0.20	1.80	3.34	11:03	-0.30	1.25	0.93
		Dt_min 11am-7pm under spray	3.09	2.59	1.58	0.07	0.79	3.34	11:03	0.01	1.68	0.74
		Dt_avg 11am-7pm under spray	0.35	-0.17	-0.83	-2.55	1.00	0.79	14:01	-2.65	-0.95	0.69
		Dt_max 11am-7pm under spray	0.36	-0.05	-0.82	-2.29	0.86	0.79	14:01	-2.47	-0.85	0.62
		Dt_avg 11am-7pm under spray	1.41	1.02	0.07	-0.85	0.92	1.58	11:03	-1.06	0.18	0.59
		Dt_max 11am-7pm under spray	1.47	1.13	0.41	-0.73	0.84	1.58	11:03	-0.92	0.41	0.53

Table 7
Daily humidification statistics. Refer to Table 5 as for the icons meaning.

	DATE	LOGIC	Percentiles				MAX	When?	MIN	AVG	DEV.S	
			99°	90°	50°	1°						
ANCONA MONITORING CAMPAIGN	13/Jul	ON-OFF	71.18	64.21	56.80	46.88	6.55	72.71	19:55	44.92	57.35	5.19
	14/Jul	ON-OFF	73.76	68.31	52.72	40.82	12.35	81.41	10:06	39.16	54.49	8.78
	15/Jul	ON-OFF	92.45	83.03	64.06	49.72	10.98	93.31	19:33	46.03	66.17	9.97
	13/Aug	FUZZY	75.33	70.71	61.26	51.86	9.47	77.90	17:50	48.05	62.25	6.00
	15/Aug	FUZZY	72.22	64.33	56.97	52.92	4.47	77.92	12:41	52.03	58.33	4.53
	16/Aug	FUZZY	66.67	63.52	55.27	47.22	5.83	69.76	10:22	45.46	56.00	4.61
	17/Aug	FUZZY	66.53	64.00	60.88	53.93	5.02	68.49	13:40	53.55	60.14	3.18
	18/Aug	FUZZY	74.38	70.81	67.68	60.79	2.71	79.10	19:33	58.24	67.71	2.55
	19/Aug	FUZZY	83.36	79.27	67.03	57.80	9.32	84.22	11:02	56.13	68.35	6.52
ROME MONITORING CAMPAIGN	24/Aug	NO STOP	63.19	57.47	49.08	39.22	9.09	65.03	11:35	37.97	49.35	5.96
	25/Aug	NO STOP	76.53	71.60	63.80	57.45	6.65	80.36	11:38	56.93	64.84	4.52
	27/Aug	NO STOP	57.49	53.79	46.99	38.65	8.03	60.41	12:12	38.09	47.17	4.94
	28/Aug	ON-OFF	59.98	55.65	47.76	47.06	5.49	61.18	11:41	47.06	50.05	3.66
	29/Aug	FUZZY	68.62	63.63	53.79	42.83	8.63	70.13	11:34	42.13	54.68	6.15
	30/Aug	FUZZY	63.98	60.12	54.53	46.96	5.50	64.44	11:45	46.43	54.81	3.92

that in the Roman park, on average), the risk for over-moisturing was non-negligible (refer to the daily statistics in Table 7). The 99th percentile of the humidity records trespassed 65% (threshold proposed by Dominguez [72]) and 70% (threshold proposed by Ishii et al. [38]) for

the 100% and the 70% of the time respectively. The median never crossed the 70% limit, but surpassed 65% for the 22.2% of the time.

In Rome, such percentages narrowed down to less than a third.

The protracted spray activations allowed by the fuzzy controller

Table 8
Cooling and humidification rate.

DATE	LOGIC	COOLING RATE	MAX	Where	When	Spray duration [s]	Spatial distribution of % occurrence					AVG	DEV.S	
							C	E	S	W	N			
HUMIDIFICATION RATE														
ANCONA MONITORING CAMPAIGN	13/Jul	ON-OFF	ΔT-/min [°C]	-1.02	E	16:27	/	13.63	16.30	26.28	18.00	25.79	-0.20	0.16
			ΔRH+/min [%]	9.55	S	18:29	/	10.39	22.34	24.94	22.60	19.74	2.51	2.14
	14/Jul	ON-OFF	ΔT-/min [°C]	-0.76	S	16:38	/	15.96	18.40	25.06	16.85	23.73	-0.20	0.14
			ΔRH+/min [%]	11.53	S	12:55	/	7.58	19.07	27.38	24.94	21.03	3.24	2.18
	15/Jul	ON-OFF	ΔT-/min [°C]	-0.99	S	18:24	/	15.84	18.81	26.73	16.58	22.03	-0.20	0.16
			ΔRH+/min [%]	10.18	S	19:13	/	9.16	22.64	28.30	19.95	19.95	2.32	1.98
	13/Aug	FUZZY	ΔT-/min [°C]	-0.96	S	12:31	240	13.72	15.21	33.17	17.96	19.95	-0.21	0.15
			ΔRH+/min [%]	13.39	S	13:37	40	9.09	15.72	30.47	20.88	23.83	3.35	2.24
	15/Aug	FUZZY	ΔT-/min [°C]	-0.52	S	15:01	50	14.37	16.17	33.53	15.57	20.36	-0.17	0.12
ROME MONITORING CAMPAIGN			ΔRH+/min [%]	10.84	S	12:41	30	5.16	21.29	36.77	19.35	17.42	2.78	2.40
	16/Aug	FUZZY	ΔT-/min [°C]	-0.72	S	16:53	60	14.29	13.91	31.20	18.80	21.80	-0.17	0.13
			ΔRH+/min [%]	10.58	W	15:40	170	9.48	16.81	35.34	18.97	19.40	2.58	2.33
	17/Aug	FUZZY	ΔT-/min [°C]	-0.94	S	18:12	60	16.13	16.67	27.42	16.13	23.66	-0.17	0.13
			ΔRH+/min [%]	11.28	C	18:47	50	12.00	16.50	35.50	22.50	13.50	1.89	1.97
	18/Aug	FUZZY	ΔT-/min [°C]	-0.40	W	13:39	80	16.67	13.33	26.67	21.43	21.90	-0.13	0.10
			ΔRH+/min [%]	8.53	S	14:44	20	8.05	20.69	35.06	21.84	14.37	1.68	1.53
	19/Aug	FUZZY	ΔT-/min [°C]	-0.48	S	11:20	30	14.73	13.18	31.78	18.60	21.71	-0.15	0.10
			ΔRH+/min [%]	7.96	E	15:20	50	5.96	21.10	39.91	16.97	16.06	1.43	1.14
24/Aug	NO STOP	ΔT-/min [°C]	-0.89	W	11:48	/	18.20	23.93	17.59	18.20	22.09	-0.24	0.16	
			ΔRH+/min [%]	13.48	C	11:20	/	16.55	26.17	17.00	16.78	23.49	4.06	2.90
	25/Aug	NO STOP	ΔT-/min [°C]	-0.98	S	10:43	/	17.24	20.23	18.85	20.00	23.68	-0.21	0.15
			ΔRH+/min [%]	12.85	S	17:59	/	14.45	20.54	20.77	15.58	28.67	3.09	2.41
	27/Aug	NO STOP	ΔT-/min [°C]	-1.05	N	12:03	/	20.25	18.18	21.28	14.05	26.24	-0.26	0.17
			ΔRH+/min [%]	21.66	E	13:40	/	14.55	18.64	28.41	19.55	18.86	5.41	3.40
28/Aug	ON-OFF	ΔT-/min [°C]	-0.87	E	15:27	/	20.25	23.21	16.88	17.30	22.36	-0.24	0.17	
			ΔRH+/min [%]	12.99	C	15:14	/	18.67	21.52	18.67	20.76	20.38	2.84	3.03
	29/Aug	FUZZY	ΔT-/min [°C]	-0.80	E	14:10	200	17.56	22.38	14.16	18.70	27.20	-0.24	0.16
30/Aug	FUZZY	ΔT-/min [°C]	-0.84	C	14:05	140	23.30	18.75	17.61	18.75	21.59	-0.21	0.14	
			ΔRH+/min [%]	11.58	C	12:04	40	15.88	23.24	21.47	15.29	24.12	3.72	2.79

increased the risk for borderline humidity levels. On the other side, as the Humidex was incorporated in the input variables, the power was cut off as soon as harmful combinations of temperature and humidity were detected. Indeed, it was with the on-off controller or under continuous operation that the absolute maxima were reached in both the locations (93.3% in Ancona, 80.4% in Rome).

The cooling and humidification rates at the different probes locations were computed too.

As apparent in Table 8, the temperature decrement, as well as the humidity increment in the time step was more attenuated under fuzzy control, thus promoting comfort and acclimatization. Both the on/off temporization and the ongoing operation resulted in steeper variations, notably under still air conditions (like those observed in Rome). In detail:

- In Ancona, the maximum temperature drop, measured in a minute time, was around 1 °C under both on-off and fuzzy operation (considering the probes' accuracy) and frequently occurred late in the afternoon. The average was 0.2 °C, hitting a low of 0.1 °C.
- In Rome, the cooling peak was again 1 °C under continuous and intermittent operation with an average of about 0.3°, while it got capped at 0.8 °C under fuzzy operation (average of 0.2 °C).
- In Ancona, the greatest variations (maximum and average) occurred at the south-located probe, basically all the times. This was the effect of the wind that blew channelled between the office and the cement wall, with a dominant component due south-west at an average speed of 2.5 m/s. On the same grounds, the mid-position and eastern-located probes were the least affected by swift changes, notably on mean basis. This demonstrates the role of local eddies in canyon-shaped contexts.

- In Rome, the degree of spatial skewness was much less appreciable, with both maximum and average values evenly distributed among the five locations, mostly because of milder winds and gusts due to the local orography. A slightly attenuated response was found again in the central location, yet in case of still air conditions, this was likely the effect of a more stable temperature in the middle of the sprayed air volume.
- In Ancona, the humidity rose by up to 13.4%, although the average was 2.4%. In Rome the average increment jumped to 3.9%, hitting a high of 5.4% under no-stop operation.
- The duration of the spray appeared to play no role in the record of maximum variations.

3.2. The role of the controller

As introduced in paragraph 2.5, fuzzy and on-off logics were directly compared over days of equivalent boundary conditions: the 13th of July and the 16th of August as for the first monitoring, the 28th and the 30th of August as for the second run.

Fig. 4 maps the time trends of the five thermohygrometers beneath the spray in Ancona. In Figs. 5 and 6 (which refer to the Roman monitoring), both the horizontal distribution and the vertical distribution are presented. The outputs of the meteorological station and of the additional probe in the church square are aggregated as well.

Fig. 4 demonstrates how the adoption of a simple temporization favored greater differences among the five monitored sub-zones beneath the spray. The south, east and center locations hit a high of about 34 °C, far beyond comfort limits. Between 5 pm and 6 pm all the sprayed area was above 30 °C. The eastern zone stayed over this value for almost all the afternoon. Conversely, as the sun went down, the

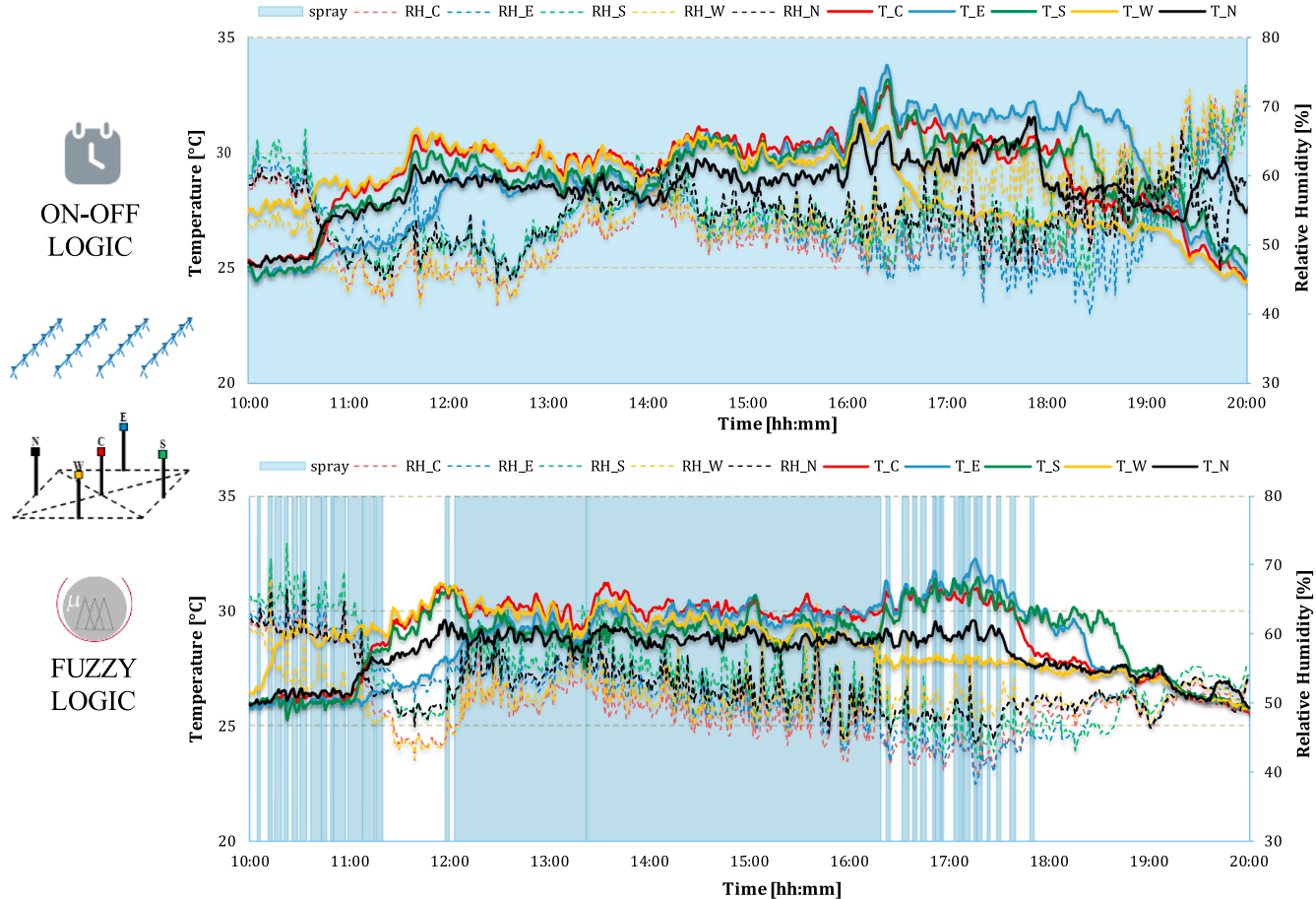


Fig. 4. Horizontal thermohygrometric map, recorded on the 13th of July (on-off logic) and on the 18th of August (fuzzy logic) in Ancona. On the leftmost side of the picture is the scheme of the probes distribution beneath the spray, which the colormap refers to.

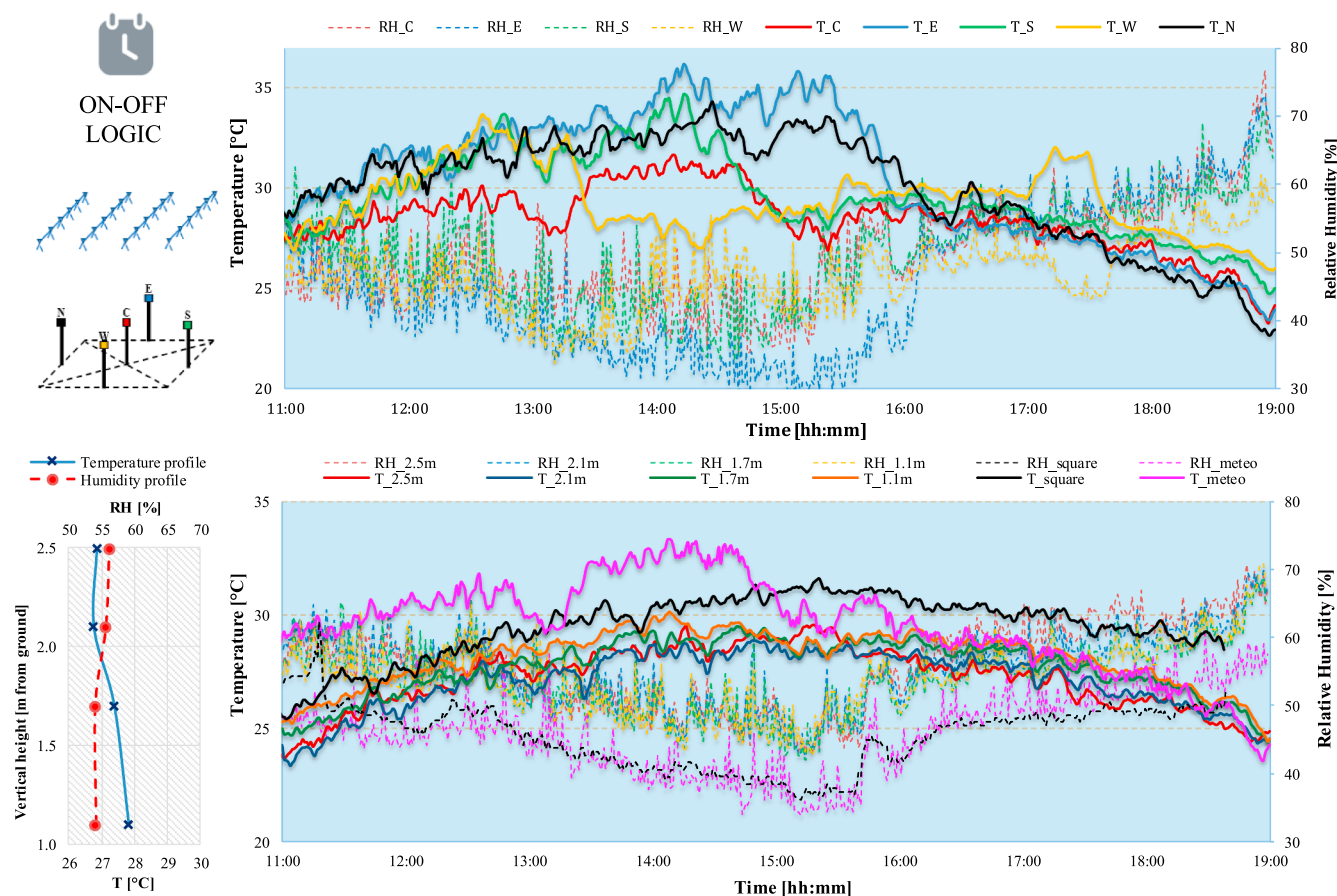


Fig. 5. Thermohygrometric map, recorded on the 28th of August (on-off logic) in Rome. The horizontal and vertical distributions are on the top and the bottom of the picture respectively. On the leftmost side are the probes distribution and the mean vertical profiles.

cooling become more effective, with the southern, central and western probes returning values below 25 °C.

With the fuzzy control on, the evolution at the different locations was much more equalized, since the logic aimed at stabilizing the lowest temperature among those recorded beneath the spray around thermal neutrality. Around 6 pm the water supply was interrupted, thus preserving the air close to 26 °C until late.

In Rome, the use of five additional probes, allowed a much deeper investigation.

Figs. 5 and 6 demonstrate that spatial thermohygrometric equalization was a fuzzy controller's prerogative again: temperatures fluctuated within a 8 °C range, while, under on-off operation, the temporal changes were accentuated (13 °C bandwidth), either in the positive and negative tracts: the temperature easily overshoot comfort boundaries, particularly at peak hours and in correspondence of the longer-sunlit eastern location, surpassing 35 °C. Conversely, from 6 pm on, the readings fell below 25 °C, with the northern, eastern and central probes returning values close to 23 °C around 7 pm.

The vertical stratification (bottom pictures in Figs. 5 and 6) was prominent under fuzzy operation, possibly because of the non-intermittent action. The average profile, charted on the leftmost side, shows that:

- under on-off operation, the air layer at 1.7 m was 0.4 °C fresher than that at 1.1 m. The maximum average temperature reduction occurred at 2.1 m (-1 °C compared to the 1.1 m measurement). The humidity didn't change substantially;
- under fuzzy operation, the air layer at 1.7 m was 1.4 °C fresher and 3.5% more humid than that at 1.1 m. The maximum temperature decrement, as well as the maximum humidity increment was

recorded at 2.1 m (-2.3 °C and +7% compared to the 1.1 m measurement).

Wind and solar radiation impinged on the time trends at the meteorological station (pink line) and in the church square (black line). The former was the hottest spot until about 3 pm: it was sunlit and benefitted neither of the wind blowing unhindered in the square nor of the nebulized water beneath the nozzles. As it sunk in the shadow of the trees, it started getting cooler while the square continued its mild warming, becoming the new hottest spot.

The pros of the mitigation technology are therefore envisaged to persist around the clock, since water mist acts upon temperature, humidity and solar radiation, all at once.

3.3. Energy and comfort performance

Energy and water consumption data are summarized in Table 4.

In the wetter and windier location (Ancona), the saving achieved by the fuzzy control over the on-off temporization was 51.2% on average, with a minimum of about 25% recorded on the hottest day and a maximum of 67.5% on the coldest and cloudiest day (when the fuzzy smartly switched off the system as soon as convenient). Direct comparison over comparable days shows that the energy and water expenditure under on-off operation was 58.8% higher.

The impact was huge in the Roman setting too, although the restricted observation window (11 am–7 pm) and the gentler wind concealed much of the fuzzy potential benefit, which manifests in the wind governance and in conditions of high relative humidity and low temperature (morning and late afternoon). Nonetheless, the mean saving surpassed 24%, hitting the maximum on the days of direct comparison

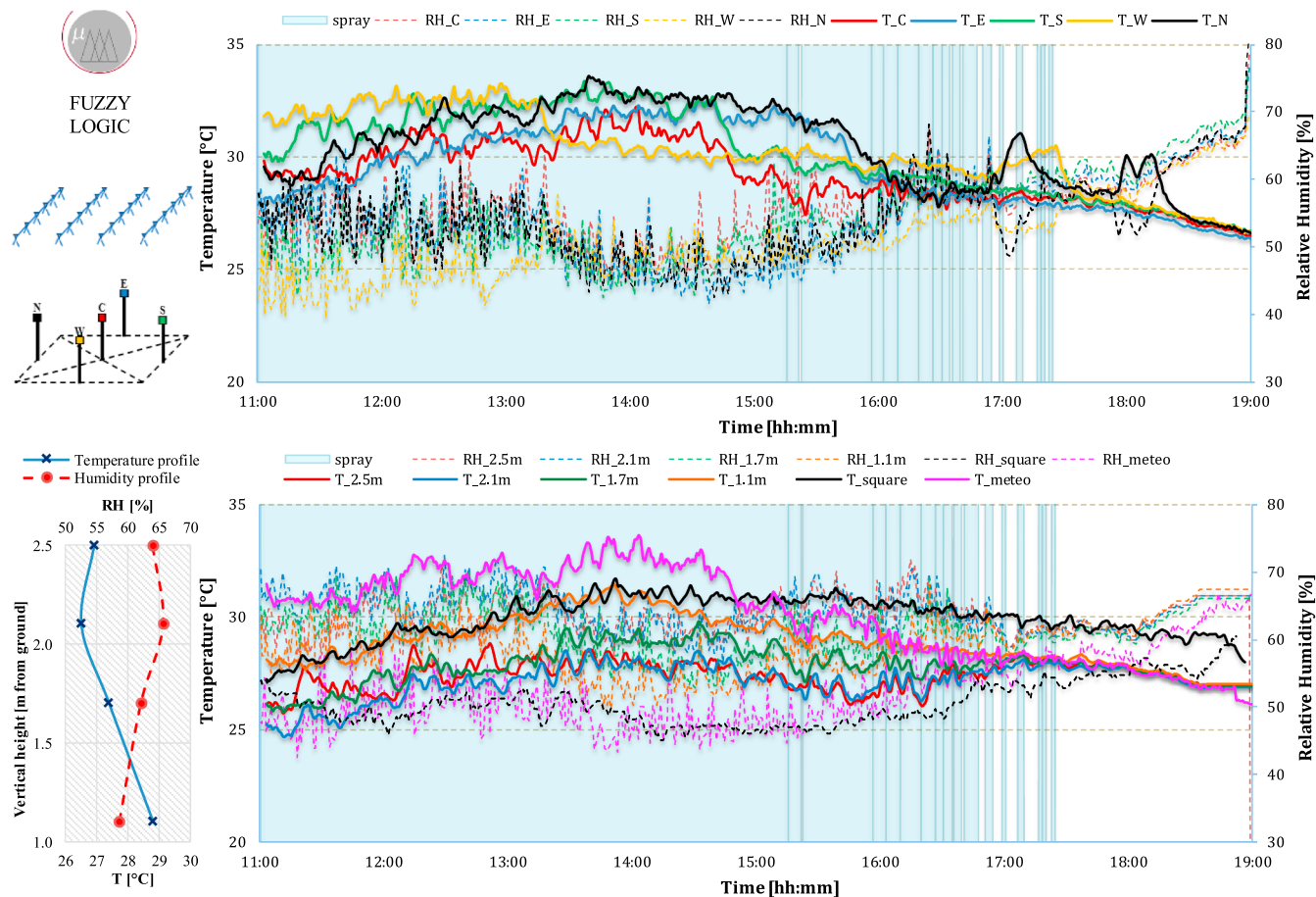


Fig. 6. Thermohygrometric map, recorded on the 30th of August (fuzzy logic) in Rome. Refer to Fig. 5 for the description.

(25.6%). The premium versus a no-stop operation was considerably higher: 49.4% on average and over 50% as ceiling.

Beyond the spectacular primary energy saving, the fuzzy achieved the best comfort performance too. To make it evident, a graphical analysis was conducted on the two days of equal thermal stress: Figs. 7 and 8 show the time evolution of the variables used to pilot the smart control (offset from neutrality in absolute terms, solar radiation, Huminex and Cooling power index) together with the relevant thresholds of incipient discomfort (refer to Table 3) and the 1-min slots over which the pump was running (light blue background). Noticeably, the logic switched off the pump on three main occasions:

- when H and PE were low, since this combination was expectedly the result of cool conditions;
- in the late afternoon, when the temperature beneath the spray was in the closest neighborhood of the neutral temperature and the sun was shaded;
- when H was in the low band and PE was hitting its upper limit. The water supply was interrupted, even over peak hours as it was inferred that, despite convenient thermohygrometric conditions, the wind was strong and thus the water mist would have likely been blown away.

It is apparent to the same extent, that the on-off logic exacerbated either unfavorable and cold environmental conditions (H close to the limit, low H and high PE combinations).

Furthermore, the difference between minimum temperature beneath the nozzles and neutral temperature was split into subsets of crescent magnitude (from a minimum of ± 0.25 °C to over 5 °C) to count the occurrence and severity of potential discomfort events (histograms in Fig. 9). If we consider the acceptable borderline at ± 2 °C from neutrality (see

Appendix), the on-off kept satisfactory conditions for the 80% of the time on the 13th of July, against the 98% reached by the fuzzy on the 18th of August. In Rome such figures incremented up to 86% and 100% on the 28th and 30th of August respectively.

Therefore, the fuzzy succeeded in preserving acceptable conditions all day long with tremendously limited electric and hydric consumptions.

3.4. Considerations on renewable energy integration

An additional benefit of energy-optimized systems is that renewable-powered configurations become a viable alternative. The main concern with high-pressure systems is that, despite the low cumulative consumption, the peak power remains quite high as dictated by the pump absorption. Nonetheless, under the fuzzy rules constraints, both power production and demand depend upon the daily sunshine hours in a form of self-compensation.

On the basis of the experimental evidence, we conceptualized a solar energy subsystem (see Fig. 10) that could power the nebulizing rack. It basically consists of a solar array (facing south, at 30°), the electronics that automatically split the production into promptly usable load and storage quota to the batteries (charge control function) and the DC/AC inverter that powers the 220 V AC water pump.

For the sunny Italian locations under test (absolute monthly mean eliophany above 8 h in summertime [73]), we assumed that the photovoltaic production could be reasonably sized to cover 2 days of autonomy [74].

We considered a total power absorption (P_{abs} in Table 9) of 1019 W (919 W from the pump and 100 W from the Sense&Act sub-system appliances – see Fig. 10) and the worst case of non-stop operation over the 10am–8 pm time slot. Once the inverter losses had been included, we computed the ampere-hour requirements to the battery system. With a Depth of

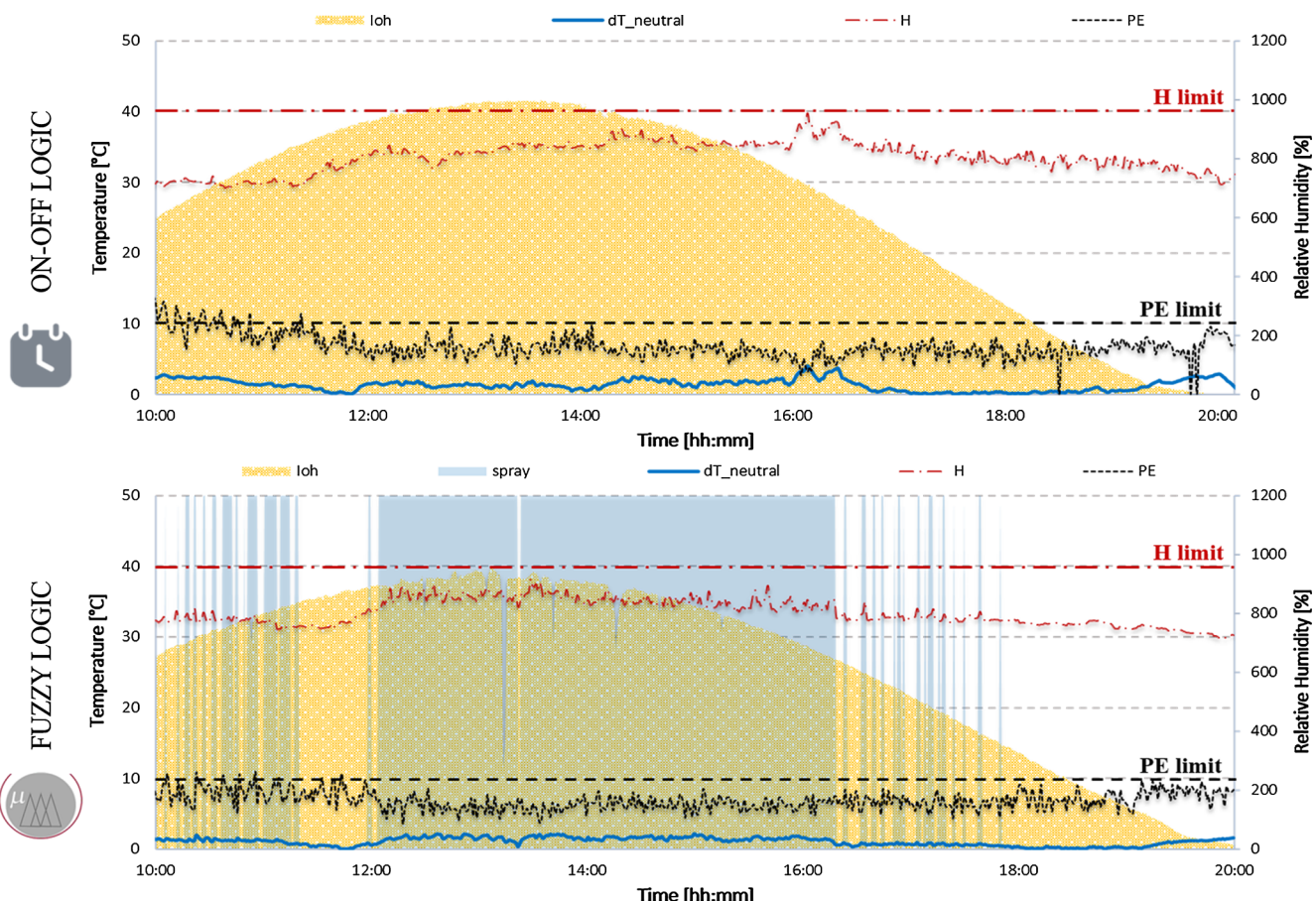


Fig. 7. Daily time trends of the inputs and output selected for the smart control: comparison of the evolution under on-off temporization and under fuzzy operation on days of equal thermal stress during the first monitoring campaign.

Discharge (DoD) of 50%, the needed capacity touched 200 Ah. A total of 5, 200 Ah, 12 V batteries sufficed to store as much power as needed for two days. Given the storage losses and the local solar availability, we estimated the number of panels over both the months of minimum and maximum daily direct sunshine availability assuming a medium-efficiency polycrystalline panel (peak power 275 W), according to the Italian market panorama [75].

With 6 panels, the nebulizing system could be solar-powered over the whole summer period and in both locations, under continuous or on-off operation, yet with potential shortcomings in case of protracted periods of overcast sky.

Such arrangement was expectedly oversized in case of fuzzy control. In fact, over both the monitoring campaigns the fuzzy controller switched on the pump for maximum 50% of the time (touching a minimum of 22% on the 15th of August).

To estimate the benefit, we replicated the calculation considering half the number of operating hours (5 h a day) as a precautionary approach. The results are highlighted in bold letters in Table 9. We concluded that 3 medium-high efficiency PV panels (or 2 high-end panels with peak power over 350 W) could suffice to power the proposed smart system with the storage endowment cut down to 3 200 Ah, 12 V batteries (2 if the autonomy was slightly reduced).

As final notice, it should be stressed that the 919 W pump could supply up to double the number of nozzles (48), thus covering a perimeter area beneath the spray of nearly 40 m².

3.5. The role of wind

The performance of the proposed system was deeply affected by the airflow patterns all around, either in terms of absolute value and of

turbulence intensity. As wind increased its speed and variability, the atomized droplets were swept away or entrained in strong eddies thus undercutting the cooling effect.

For this reason, the use of water nebulization to cool down the outdoors is generally bound to semi-enclosed spaces [28,38,74]. The selection of a proper installation site and the implementation of a wind-sensitive control logic (as the fuzzy one here proposed) is expected to widen the applicability.

This came up particularly evident, even from a quantitative point of view, while investigating the possibility to forecast the capacity of the fuzzy-controlled system to preserve high comfort standards (small offset from the neutral temperature) given the environmental boundary conditions.

To do so, an A.I.-based approach, relying upon evolutionary algorithms, was adopted to search for mathematical relationships among variables in the dataset. The offset from the neutral temperature worked as target variable, while the meteorological data and the control indices -Humidex (H) and Cooling power index (PE) - were the input variables. The original dataset was filtered to only consider the time slots over which the pump was running. Each input parameter was cleaned of its outliers by adopting a threshold of 2 multiples of the interquartile range.

The solutions were constrained by a suite of operators: beyond basic and exponential functions, the delayed variable (delay) and simple moving average (sma) functions were contemplated. 75% of the data was used to train the model, while 25% was used for validation.

Size or complexity of the equations increased along the Pareto frontier while the error dropped. Solutions with the same complexity were put into competition with each other, to preserve the one with the best fitting for that complexity. The process continued iteratively to ameliorate the squared error.

Eventually, the following 12-coefficient equation was obtained for

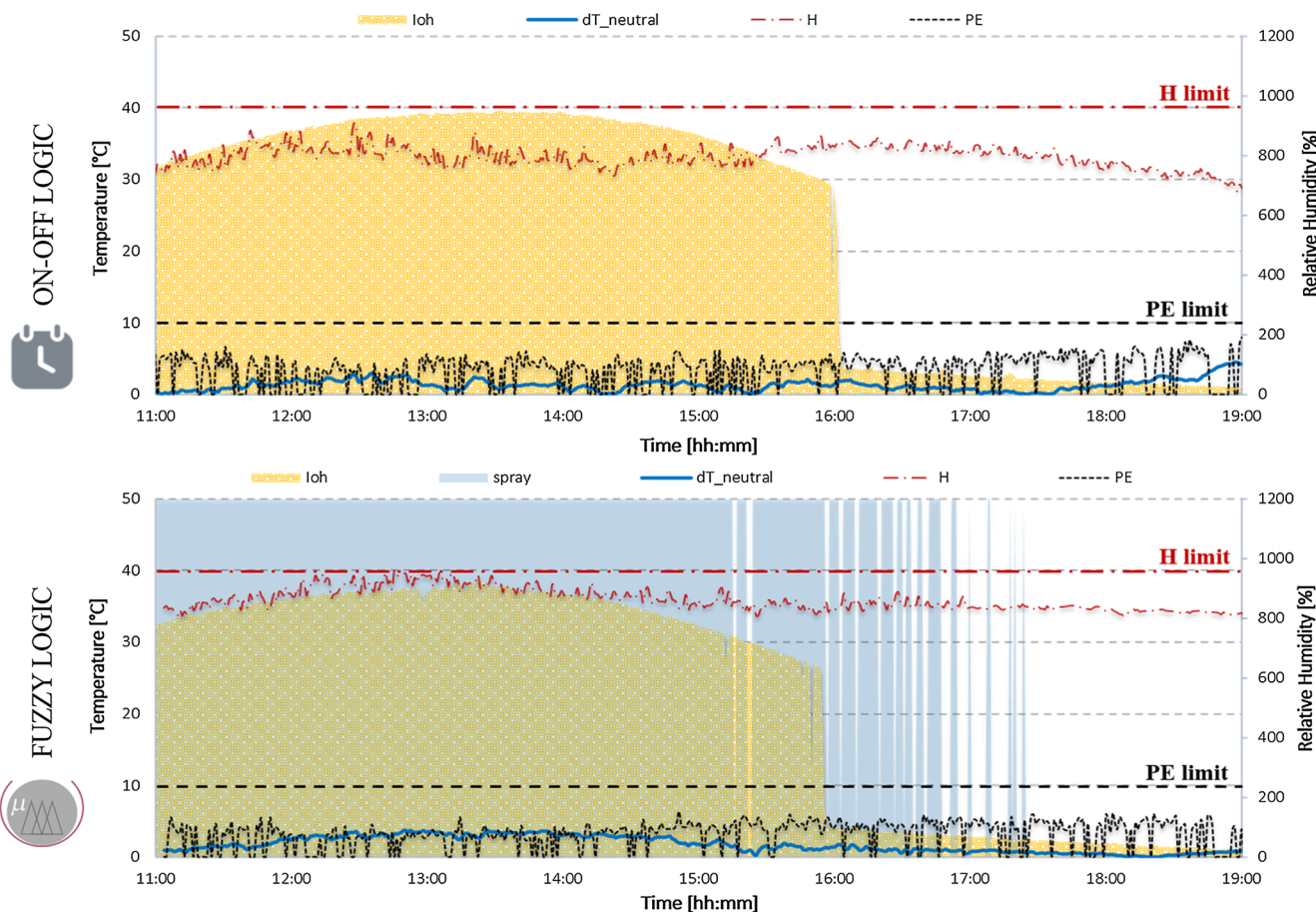


Fig. 8. Daily time trends of the inputs and output selected for the smart control: comparison of the evolution under on-off temporization and under fuzzy operation on days of equal thermal stress during the second monitoring campaign.

wind speeds greater than zero:

$$\begin{aligned} \text{Dtneutral} = & 1.104 + 1.595 \cdot \ln(\max(9.612 + 6.67 \cdot ws + 0.4004 \cdot PE^2 \\ & + 0.03509 \cdot PE \cdot ws^2 - 4.165 \cdot PE - 0.9806 \cdot ws \cdot PE, 0.4004 \cdot \\ & PE^2 / (9.612 + 6.67 \cdot ws))) - 0.1309 \cdot ws \end{aligned} \quad (9)$$

The R^2 goodness of fit approached 0.98. The maximum absolute

error was 1.3°C , while the average was -0.04°C . The mean squared error plateaued at 0.002°C^2 (see Fig. 11).

Indeed, the correlation was very precise and, unexpectedly, involved just two of the input parameters: PE and wind speed (ws in the equation). Since PE is a function of wind speed and air temperature beneath the sprays, it could be inferred that such parameters were governing variables for the spray cooling capacity. This implies that a

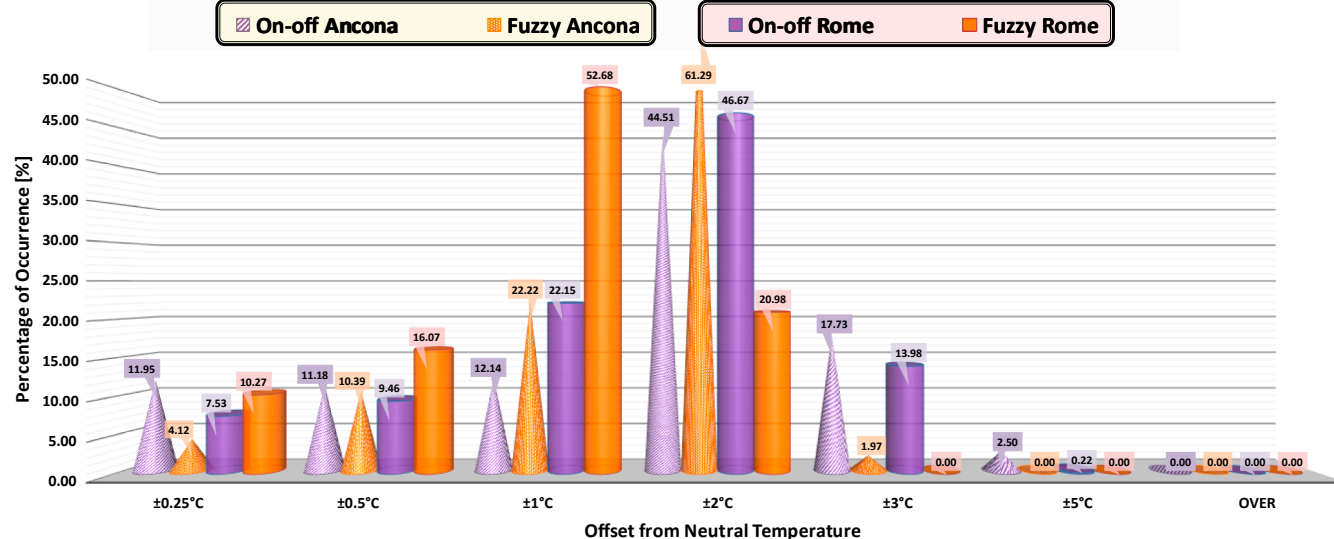


Fig. 9. Histograms of occurrence: percentage of how many times the offset between minimum temperature beneath the spray and neutral temperature fell in subsets of crescent magnitude (from $< \pm 0.25^\circ\text{C}$ to over 5°C).

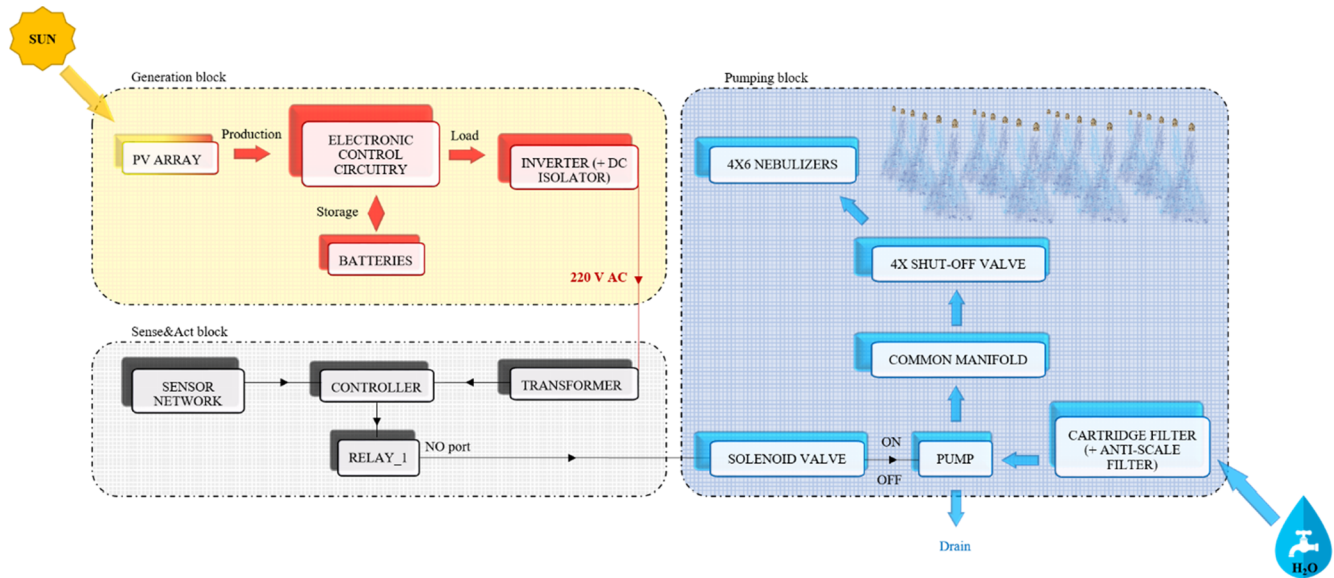


Fig. 10. Schematics of the generation, control and pumping sub-systems with reciprocal interplays.

very limited number of probes (two sensors in total) might suffice to replicate the fine control of the proposed fuzzy system.

Besides, since no history-related operator features in the equation, it was demonstrated that the spraying operation was dependent on the very concomitant values of the environmental variables.

To get the relative impact within the model of the governing variables x (ws and PE in this case) on the target variable z ($Dt_{neutral}$), a sensitivity analysis was conducted, hence the following equation was applied to all input data points.

$$\left| \frac{\partial z}{\partial x} \right| \cdot \frac{\sigma(x)}{\sigma(z)} \quad (7)$$

The main results are summarized in [Table 10](#). The fields named “%+” and “%−” represent the percent likelihood that at positive ∂z would correspond a positive or negative ∂z respectively. Cooling power index and wind speed exhibited contrasting trends: about 80% of the time PE increased or, equivalently, ws decreased, the offset from the neutral temperature narrowed down, meaning that higher air temperatures were likely to favor more incisive cooling, as discussed in paragraph 4.1.

The magnitude of the negative impact was quite different between the two independent variables, with PE's almost two times that of wind speed. The positive impact difference was much less pronounced.

Although the need for additional measuring equipment might seem a blowback compared to a simple temporization, the positive implications should be contemplated as well.

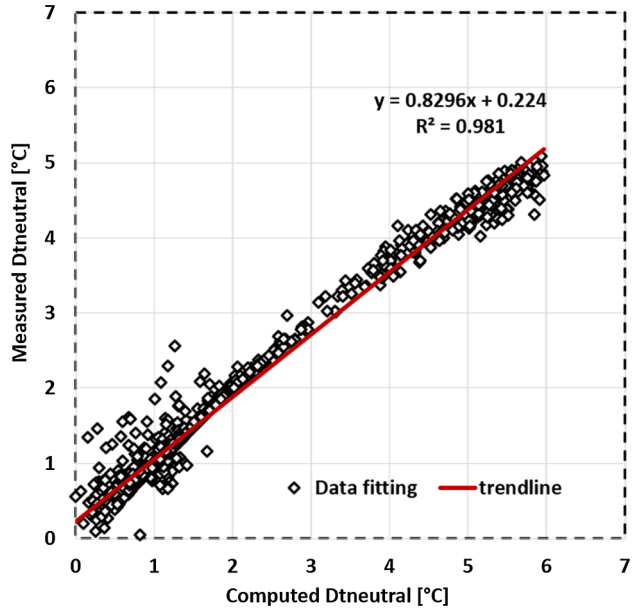


Fig. 11. Measured over computed offset from neutrality: goodness of fit.

Table 9
PV subsystem size estimation.

Load	Inverter					
Voltage [V]	P _{abs} [W]	t _{on/day} [h]	E _{abs/day} [Wh]	η	Capacity [W]	Input [Wh]
220	1019	10	10,190	0.93	947.67	10903.3
220	1019	5	5095	0.93	947.67	5451.65
Battery	Sizing and selection					
P _{nominal} [Ah]	P _{actual} [Ah]	Autonomy [d]	Capacity [Ah]	[Ah]	[V]	# _{nominal}
49.6	0.5	99.1	2	200	12	4.25
24.8	0.5	49.6	2	200	12	2.12
# _{actual}	5					0.9
η						
Panels	Sizing and selection					
E _{module} [Wh]	Monthly mean eliophany [h]	P _{module} [W]	# _{nominal}	# _{actual}		
11322.2	Min - September (both locations)	8	5.15	6	PV Panel Series GALILEO 275 Polycrystalline module	
	Max - July (Rome)	11	3.74	4		
5661.1	Min - September (both locations)	8	2.57	3	Peak Power [Wp]	
	Max - July (Rome)	11	1.87	2	275	

Table 10
Results of the sensitivity analysis.

Variable	Sensitivity	% +	+ Magnitude	% -	- Magnitude
PE	1.6606	21%	1.0492	79%	1.8219
ws	1.3239	82%	1.384	18%	1.0445

Urban metabolism research is thriving nowadays, yet data availability and quality are pre-conditions for a substantiated methodological approach [15]. Most city-scale studies, to date, rely on approximations, typically pursued by downscaling flows and stocks on the basis of population share, surface share or weighted composite factors. The supply of remote sensing data offers an efficient way to overcome such restrictions [76]. Indeed, urban planning is recently benefitting from extremely high-resolution data, captured from a diffuse sensing framework made of mobile phones, public cameras, satellites, drones, ICT data from utilities, smart meters and home automation. Coupling local mitigation technologies with sensing instruments contributes to the collection of fine-grained information useful for models training and optimization processes.

4. Conclusions

An experimental study was conducted on a novel technology that combines water nebulization and fuzzy logic to attain outdoor thermal comfort in urban open spaces. The design and functionalities were fully optimized to attain a ponderable cooling action, provide adequate climate adaptability and allow for immediate, large-scale implementation at minimum resource and bureaucratic costs.

The proposed multi-row, horizontal rack of 6×4 micro-nebulizers covered an area of approximately $3\text{ m} \times 6\text{ m}$ in plan. The nozzles were suspended at about 3 m above the ground.

The pump kept the water flow under a stable high pressure (70 bar) resulting in a 1.5 l/min supply.

The controller was indoctrinated with four inputs: the offset from the neutral air temperature, the solar radiation, the Humidex (a linear index that correlates air temperature and relative humidity) and the Cooling power index (that combines temperature and wind speed to quantify the resulting cooling potential). Linguistic terms and membership functions were assigned to each variable, thus resulting in a total of 300 customized rules aimed at avoiding nebulization any time useless (too windy) or counterproductive (too humid or too cold).

The prototype was monitored in two contexts:

- on the Marche Polytechnic University terrace (Ancona, Italy, Cfa climatic conditions), over 9 days in the hottest months (July and August);
- in a 50mx16m playground in the Centocelle district (Rome, Italy, Csa climatic conditions), over 6 clear, hot days in August.

In this way, we could verify the performance in different urban textures and climatic frames. The fuzzy logic was compared to alternative solutions, namely the on-off temporization and the continuous operation, which represent the standard.

The sensor network consisted of a meteorological station used as reference for the cooling calculations, 5 miniaturized thermohygrometers distributed at the center and mid-points of the ground-projected perimeter of the spraying rack and a rain detector. In Rome five additional temperature and humidity probes were installed to record the vertical profile under the spray and check on a 100 m distant undisturbed location.

The main results can be summarized as follows:

- In Ancona, the maximum cooling (-7.4°C , 99th percentile close to 7°C) was observed on the hottest day (mean temperature of 32.6°C). The same happened under on-off control: with 33.3°C on average, the maximum temperature drop touched 7.5°C . Both maxima occurred around 11:30 am.

- In Rome, the maximum temperature drop ranged between 3.3°C and 4.4°C , detected as soon as the system was activated or over peak hours (around 2 pm). Much greater drops were recorded under on-off operation (maximum of 6.1°C , 99th percentile above 5.5°C). This was not a pro of the control logic, but the outcome of its incapacity to switch off the pump when evaporative cooling was unnecessary. In fact, with the on-off, the temperature could drop below 25°C , causing discomfort and undue energy and water consumption.
- In terms of humidification, during both the monitoring campaigns, the median of the relative humidity distribution never went over 70%. In Rome (10% less humid than Ancona on average) the relative humidity in the whole cooled area stayed below 65% on average. Anyway, by incorporating the Humidex among the control variables, potentially uncomfortable combinations of temperature and humidity were automatically prevented.
- In both the experimental settings, the cooling rate (maximum temperature drop, measured in a minute time) slightly varied in the range -0.8°C to -1°C . The minima corresponded to the fuzzy control, which promoted softer fluctuations and milder spatial differences.
- The vertical temperature profile was not monotonically increasing, moving away from the nozzle orifice: it peaked at about 2 m above the ground (-2.3°C under fuzzy logic and -1°C under on-off control compared to the 1.1 m measurement).
- In terms of consumption, in the wetter and windier location (Ancona), the electric and hydric saving achieved by the fuzzy over the on-off logic was 51.2% on average, peaking at 67.5% on the coldest and cloudiest day (when the fuzzy smartly switched off the system as soon as convenient). At equal boundary conditions the premium touched the 60%. In Rome, the mean saving surpassed 24%, but it was calculated against a semi-undisturbed location (only 16 m away from the nebulized area) and in a narrower time window, neglecting the colder frames of the day when the fuzzy strongly manifested its merits.
- In terms of comfort, the temperature never deviated from neutrality by more than $\pm 2^\circ\text{C}$ with the fuzzy logic, while the on-off control caused this threshold to be surpassed nearly 20% of the time in Ancona and over 14% in Rome.
- Given the inclusion of solar radiation in the fuzzy logic and its capacity to strongly curb the number of operating hours, we estimated that the size of a photovoltaic system used to power the nebulizers could be halved compared to that required by an on/off or continuous operation, with much less chances of underproduction.
- Based on genetic algorithms, a 12-coefficient equation was obtained to correlate the temperature offset from neutrality, guaranteed by the fuzzy logic, with the concomitant weather conditions. With an R^2 close to 0.98 we demonstrated that the ability of the fuzzy controller in preserving comfortable conditions was largely a function of the instantaneous value of wind speed and air temperature beneath the spray. Thus, a very limited number of sensors might suffice to replicate the high-performance system here proposed.

All things considered, this study advocates on the basis of extensive experimental evidence, that fuzzy controlled water nebulization succeeds in preserving outdoor thermal comfort in urban spaces all day long in a variety of climatic conditions with tremendously limited electric and hydric consumptions compared to the conventional on-off regulation.

The energy and cost-effectiveness of the prototype, together with its climate adaptability, could pave the way for extensive implementation.

Acknowledgments

Authors warmly thank the Italian national agency for new technologies, energy and sustainable economic development (ENEA) - under the funding PAR 2017 sub-project D.6 Sviluppo di un modello integrato di smart district urbano - for providing the resources to build the prototype and for taking care of the monitoring authorizations.

Appendix

INPUT VARIABLES		
Name	Range	Number of membership functions
DTneutral	0 > 25	5
Membership function	Shape	Points
NEGLIGIBLE	Trapezoid	0 ; 0 ; 0,25 ; 0,5
COMFORTABLE	Trapezoid	0,25 ; 0,5 ; 0,75 ; 1
ACCEPTABLE	Trapezoid	0,75 ; 1 ; 2 ; 2,25
SLIGHTLY UNCOMFORTABLE	Trapezoid	2 ; 2,25 ; 2,75 ; 3
UNCOMFORTABLE	Trapezoid	2,75 ; 3 ; 25 ; 25
Ioh	-10 > 1200	3
Membership function	Shape	Points
CLOUDY	Trapezoid	-10 ; -10 ; 150 ; 200
PARTLY CLOUDY	Trapezoid	150 ; 200 ; 350 ; 400
SUNNY	Trapezoid	350 ; 400 ; 1200 ; 1200
HUMIDEX	20 > 54	5
Membership function	Shape	Points
LITTLE TO NO DISCOMFORT	Trapezoid	20 ; 20 ; 29 ; 30
ACCEPTABLE DISCOMFORT	Trapezoid	29 ; 30 ; 35 ; 36
SLIGHT DISCOMFORT	Trapezoid	35 ; 36 ; 39 ; 40
GREAT DISCOMFORT	Trapezoid	39 ; 40 ; 44 ; 45
DANGER	Trapezoid	44 ; 45 ; 54 ; 54
PE	-15 > 40	4
Membership function	Shape	Points
HOT	Trapezoid	-15 ; -15 ; 4 ; 5
MILD	Trapezoid	4 ; 5 ; 10 ; 11
COOL	Trapezoid	10 ; 11 ; 15 ; 16
COLD	Trapezoid	15 ; 16 ; 40 ; 40
Output variable		
Name	Range	Number of membership functions
SPRAY	0 > 1	2
Membership function	Shape	Points
ON	Singleton	1
OFF	Singleton	0
Defuzzification method: Center of Area		

References

- [1] IPCC. Fifth assessment report (AR5); 2018.
- [2] Livada I, Synnefa A, Haddad S, Paolini R, Garshasbi S, Ulpiani G, et al. Time series analysis of ambient air-temperature during the period 1970–2016 over Sydney, Australia. *Sci Total Environ* 2019;648:1627–38. <https://doi.org/10.1016/j.scitotenv.2018.08.144>.
- [3] Santamouris M, Cartalis C, Synnefa A, Kolokotsa D. On the impact of urban heat island and global warming on the power demand and electricity consumption of buildings—A review. *Energy Build* 2015;98:119–24. <https://doi.org/10.1016/j.enbuild.2014.09.052>.
- [4] Tremeac B, Bousquet P, de Munck C, Pigeon G, Masson V, Marchadier C, et al. Influence of air conditioning management on heat island in Paris air street temperatures. *Appl Energy* 2012;95:102–10. <https://doi.org/10.1016/j.apenergy.2012.02.015>.
- [5] Santamouris M. Cooling the buildings – past, present and future. *Energy Build* 2016;128:617–38. <https://doi.org/10.1016/j.enbuild.2016.07.034>.
- [6] Li C, Zhou J, Cao Y, Zhong J, Liu Y, Kang C, et al. Interaction between urban microclimate and electric air-conditioning energy consumption during high temperature season. *Appl Energy* 2014;117:149–56. <https://doi.org/10.1016/j.apenergy.2013.11.057>.
- [7] Radhi H, Sharples S. Quantifying the domestic electricity consumption for air-conditioning due to urban heat islands in hot arid regions. *Appl Energy* 2013;112:371–80. <https://doi.org/10.1016/j.apenergy.2013.06.013>.
- [8] Lam TNT, Wan KKW, Wong SL, Lam JC. Impact of climate change on commercial sector air conditioning energy consumption in subtropical Hong Kong. *Appl Energy* 2010;87:2321–7. <https://doi.org/10.1016/j.apenergy.2009.11.003>.
- [9] Toparlar Y, Blocken B, Maihue B, van Heijst GJF. Impact of urban microclimate on summertime building cooling demand: A parametric analysis for Antwerp, Belgium. *Appl Energy* 2018;228:852–72. <https://doi.org/10.1016/j.apenergy.2018.06.110>.
- [10] Xu X, González JE, Shen S, Miao S, Dou J. Impacts of urbanization and air pollution on building energy demands — Beijing case study. *Appl Energy* 2018;225:98–109. <https://doi.org/10.1016/j.apenergy.2018.04.120>.
- [11] Zinzi M, Carnielo E, Mattoni B. On the relation between urban climate and energy performance of buildings. A three-years experience in Rome, Italy. *Appl Energy* 2018;221:148–60. <https://doi.org/10.1016/j.apenergy.2018.03.192>.
- [12] Santamouris M. On the energy impact of urban heat island and global warming on buildings. *Energy Build* 2014;82:100–13. <https://doi.org/10.1016/j.enbuild.2014.07.022>.
- [13] Liang Z, Tian Z, Sun L, Feng K, Zhong H, Gu T, et al. Heat wave, electricity rationing, and trade-offs between environmental gains and economic losses: The example of Shanghai. *Appl Energy* 2016;184:951–9. <https://doi.org/10.1016/j.apenergy.2016.06.045>.
- [14] UN. Adoption of the Paris agreement. In: United Nations Framework Conv. Clim. Chang. Paris; 2015. p. 31.
- [15] Dijst M, Worrell E, Böcker L, Brunner P, Davoudi S, Geertman S, et al. Exploring urban metabolism—Towards an interdisciplinary perspective. *Resour Conserv Recycl* 2018;132:190–203. <https://doi.org/10.1016/j.resconrec.2017.09.014>.
- [16] McCarthy MP, Best MJ, Betts RA. Climate change in cities due to global warming and urban effects. *Geophys Res Lett* 2010. <https://doi.org/10.1029/2010GL042845>.
- [17] Qian S, Geng Y, Wang Y, Ling J, Hwang Y, Radermacher R, et al. A review of elastocaloric cooling: Materials, cycles and system integrations. *Int J Refrig* 2016;64:1–19. <https://doi.org/10.1016/j.ijrefrig.2015.12.001>.
- [18] Sun R, Chen A, Chen L, Lü Y. Cooling effects of wetlands in an urban region: The case of Beijing. *Ecol Indic* 2012;20:57–64. <https://doi.org/10.1016/j.ecolind.2012.02.006>.
- [19] Efthymiou C, Santamouris M, Kolokotsa D, Koras A. Development and testing of photovoltaic pavement for heat island mitigation. *Sol Energy* 2016. <https://doi.org/10.1016/j.solener.2016.01.054>.
- [20] Raman AP, Anoma MA, Zhu L, Rephaeli E, Fan S. Passive radiative cooling below ambient air temperature under direct sunlight. *Nature* 2014. <https://doi.org/10.1038/nature13883>.
- [21] Santamouris M, Ding L, Fiorito F, Oldfield P, Osmond P, Paolini R, et al. Passive and active cooling for the outdoor built environment – Analysis and assessment of the cooling potential of mitigation technologies using performance data from 220 large scale projects. *Sol Energy* 2017;154:14–33. <https://doi.org/10.1016/j.solener.2016.12.006>.
- [22] Synnefa A, Santamouris M, Akbari H. Estimating the effect of using cool coatings on energy loads and thermal comfort in residential buildings in various climatic conditions. *Energy Build* 2007. <https://doi.org/10.1016/j.enbuild.2007.01.004>.
- [23] Paolini R, Zinzi M, Poli T, Carnielo E, Mainini AG. Effect of ageing on solar spectral reflectance of roofing membranes: Natural exposure in Roma and Milano and the impact on the energy needs of commercial buildings. *Energy Build* 2014;84:333–43. <https://doi.org/10.1016/j.enbuild.2014.08.008>.
- [24] Mastrapostoli E, Santamouris M, Kolokotsa D, Vassilis P, Venieri D, Gompakis K. On the ageing of cool roofs: Measure of the optical degradation, chemical and biological analysis and assessment of the energy impact. *Energy Build* 2016. <https://doi.org/10.1016/j.enbuild.2015.05.030>.
- [25] Dombrovsky LA, Solovjov VP, Webb BW. Attenuation of solar radiation by a water mist from the ultraviolet to the infrared range. *J Quant Spectrosc Radiat Transf* 2011;112:1182–90. <https://doi.org/10.1016/j.jqsrt.2010.08.018>.
- [26] Narumi D, Shigematsu K, Shimoda Y. Effect of the evaporative cooling techniques by spraying mist water on reducing urban heat flux and saving energy in apartment house. In: 2nd Int. Conf. Countermeas. to Urban Heat Islands, 7; 2009. p. 175–81.
- [27] Nishimura N, Nomura T, Iyota H, Kimoto S. Novel water facilities for creation of comfortable urban micrometeorology. *Sol Energy* 1998;64:197–207. [https://doi.org/10.1016/S0038-092X\(98\)00116-9](https://doi.org/10.1016/S0038-092X(98)00116-9).
- [28] Farmham C, Nakao M, Nishioka M, Nabeshima M, Mizuno T. Study of mist-cooling for semi-enclosed spaces in Osaka, Japan. *Procedia Environ Sci* 2011;4:228–38. <https://doi.org/10.1016/j.proenv.2011.03.027>.
- [29] Yoon GHY. Study on a cooling system using water mist sprayers; system control considering outdoor environment, Korea-Japan Jt. Symp. Human-Environment Syst. Cheju, Korea; 2008. p. 4.
- [30] Montazeri H, Toparlar Y, Blocken B, Hensen JLM. Simulating the cooling effects of water spray systems in urban landscapes: A computational fluid dynamics study in Rotterdam, The Netherlands. *Landsd Urban Plan* 2017;159:85–100. <https://doi.org/10.1016/j.landurbplan.2016.10.001>.
- [31] Nunes J, Zoiio I, Jacinto N, Nunes A, Campos T, Pacheco M, Fonseca D. Misting-cooling systems for microclimatic control in public space. Available through <<http://Www.Proap.Pt/847/Misting-Cooling-Systemsfor-Microclim>>; 2016.
- [32] Dominguez FJS, Alvarez S, de la Flor. The effect of evaporative techniques on reducing urban heat, Santamouris, M., Kolokotsa, D. *Urban Clim. Mitig. Tech.* Routledge, London; 2016.
- [33] Kolokotroni M, Giannitsaris I, Watkins R. The effect of the London urban heat island on building summer cooling demand and night ventilation strategies. *Sol Energy* 2006;80:383–92. <https://doi.org/10.1016/j.solener.2005.03.010>.
- [34] Paolini R, Zani A, MeshkinKia M, Castaldo VL, Pisello AL, Antretter F, et al. The hygrothermal performance of residential buildings at urban and rural sites: Sensible and latent energy loads and indoor environmental conditions. *Energy Build* 2017;152. <https://doi.org/10.1016/j.enbuild.2016.11.018>.
- [35] Salamanca F, Georgescu M, Mahalov A, Moustaqi M, Wang M. Anthropogenic heating of the urban environment due to air conditioning. *J Geophys Res Atmos* 2014;119:5949–65. <https://doi.org/10.1002/2013JD021225>.
- [36] Atieh A, Al Shariff S. Solar energy powering up aerial misting systems for cooling surroundings in Saudi Arabia. *Energy Convers Manage* 2013;65:670–4. <https://doi.org/10.1016/j.enconman.2011.10.031>.
- [37] Yoon G, Yamada H, Okumiya M. Study on a cooling system using water mist sprayers; system control considering outdoor environment. Korea-Japan Jt. Symp. Human-Environment Syst. Cheju, Korea; 2008. p. 4.
- [38] Ishii T, Tsujimoto M, Yoon G, Okumiya M. Cooling system with water mist sprayers for mitigation of heat-island drymist system : Uchimizu; 2009. p. 2–3.
- [39] Kang D, Strand RK. Performance control of a spray passive down-draft evaporative cooling system. *Appl Energy* 2018;222:915–31. <https://doi.org/10.1016/j.apenergy.2018.03.039>.
- [40] Mora C, Dousset B, Caldwell IR, Powell FE, Geronimo RC, Bielecki CR, et al. Global risk of deadly heat. *Nat Clim Chang* 2017;7:501–6. <https://doi.org/10.1038/nclimate3322>.
- [41] Holterman HJ. Kinetics and evaporation of water drops in air; 2003.
- [42] Montazeri H, Blocken B, Hensen JLM. CFD analysis of the impact of physical parameters on evaporative cooling by a mist spray system. *Appl Therm Eng* 2015;75:608–22. <https://doi.org/10.1016/j.applthermaleng.2014.09.078>.
- [43] ANSYS Inc, ANSYS FLUENT 12.0 User's Guide; 2009.
- [44] Köppen W, Geiger R. Das Geographische System der Klimate, Handb. Der Klimatologie; 1936.
- [45] ISO. ISO 7726:1998 Ergonomics of the thermal environment – Instruments for measuring physical quantities; 1998.
- [46] Farmham C, Nakao M, Nishioka M, Nabeshima M, Mizuno T. Effect of water temperature on evaporation of mist sprayed from a nozzle. *J Heat Isl Inst Int* 2015;10:35–44.
- [47] Chaker M, Meher-Homji CB, Mee T. Inlet fogging of gas turbine engines—Part II: Fog droplet sizing analysis, nozzle types, measurement, and testing. *J Eng Gas Turbines Power* 2004. <https://doi.org/10.1115/1.1712982>.
- [48] Li X, Kang S, Zhang G, Qu B, Tripathee L, Paudyal R, et al. Light-absorbing impurities in a southern Tibetan Plateau glacier: Variations and potential impact on snow albedo and radiative forcing. *Atmos Res* 2018;200:77–87. <https://doi.org/10.1016/j.atmosres.2017.10.002>.
- [49] Yan H, Pan Y, Li Z, Deng S. Further development of a thermal comfort based fuzzy logic controller for a direct expansion air conditioning system. *Appl Energy* 2018;219:312–24. <https://doi.org/10.1016/j.apenergy.2018.03.045>.
- [50] Zadeh LA. Fuzzy sets. *Inf Control* 1964;8(3):338–53.
- [51] Ulpiani G, Borgognoni M, Romagnoli A, Di Perna C. Comparing the performance of on/off, PID and fuzzy controllers applied to the heating system of an energy-efficient building. *Energy Build* 2016;116. <https://doi.org/10.1016/j.enbuild.2015.12.027>.
- [52] Ulpiani G, Benedettelli M, di Perna C, Naticchia B. Overheating phenomena induced by fully-glazed facades: Investigation of a sick building in Italy and assessment of the benefits achieved via model predictive control of the AC system. *Sol Energy* 2017;157. <https://doi.org/10.1016/j.solener.2017.09.009>.
- [53] Ulpiani G. Overheating phenomena induced by fully-glazed facades: Investigation of a sick building in Italy and assessment of the benefits achieved via fuzzy control of the AC system. *Sol Energy* 2017;158:572–94. <https://doi.org/10.1016/j.solener.2017.10.024>.
- [54] Babuska R, Verbruggen HB. An overview of fuzzy modeling for control. *Control Eng Pract* 1996;4:1593–606. [https://doi.org/10.1016/0967-0661\(96\)00175-X](https://doi.org/10.1016/0967-0661(96)00175-X).
- [55] Coccolo S, Kampf J, Scartezzini JL, Pearlmuter D. Outdoor human comfort and thermal stress: A comprehensive review on models and standards. *Urban Clim* 2016;18:33–57. <https://doi.org/10.1016/j.uclim.2016.08.004>.
- [56] Salata F, Golasi I, de Lieto Vollaro R, de Lieto Vollaro A. Outdoor thermal comfort in the Mediterranean area. A transversal study in Rome, Italy. *Build Environ*

- 2016;96:46–61. <https://doi.org/10.1016/j.buildenv.2015.11.023>.
- [57] Rutty M, Scott D, Johnson P, Jover E, Pons M, Steiger R. Behavioural adaptation of skiers to climatic variability and change in Ontario, Canada. *J Outdoor Recreatour* 2015;11:13–21. <https://doi.org/10.1016/j.jort.2015.07.002>.
- [58] Masterton JM, Richardson FA. Humidex: a method of quantifying human discomfort due to excessive heat and humidity (Internet). Canada: Ministere de l'Environnement 1979. n.d.
- [59] Santee WR, Wallace RF. Comparison of weather service heat indices using a thermal model. *J Therm Biol* 2005. <https://doi.org/10.1016/j.jtherbio.2004.07.003>.
- [60] Santee WR, Wallace RF. Use of Humidex to set thermal work limits for emergency workers in protective clothing (No. M05-21). ARMY RESEARCH INST OF ENVIRONMENTAL MEDICINE NATICK MA BIOPHYSICS AND BIOMEDICAL MODELING DIV; 2005.
- [61] Lavalle C. Pan European assessment of weather driven natural risks; 2006.
- [62] d'Ambrosio Alfano FR, Palella Bl, Riccio G. Thermal environment assessment reliability using temperature —humidity indices. *Ind Health* 2011;49:95–106. <https://doi.org/10.2486/indhealth.MS1097>.
- [63] Vinje TE. The cooling power in Antarctica. *Nor. Polarinstitt Arb*. 1961;22.
- [64] Gomez F, Gil L, Montero L, de Vicente V. Climate indicators for cities, Sustain. City Iii Urban Regen. Sustain 2004;18:91–102.
- [65] Balaras C, Tselepidaki I, Santamouris M, Asimakopoulos D. Calculations and statistical analysis of the environmental cooling power index for Athens, Greece. *Energy Convers Manage* 1993;34:139–46. [https://doi.org/10.1016/0196-8904\(93\)90155-4](https://doi.org/10.1016/0196-8904(93)90155-4).
- [66] Santamouris M, Gaitani N, Spanou A, Saliari M, Giannopoulou K, Vasilakopoulou K, et al. Using cool paving materials to improve microclimate of urban areas - Design realization and results of the flisvos project. *Build Environ* 2012;53:128–36.
- <https://doi.org/10.1016/j.buildenv.2012.01.022>.
- [67] Gómez F, Gil L, Jabaloyes J. Experimental investigation on the thermal comfort in the city: Relationship with the green areas, interaction with the urban microclimate. *Build Environ* 2004;39:1077–86. <https://doi.org/10.1016/j.buildenv.2004.02.001>.
- [68] Gómez F, Tamarit N, Jabaloyes J. Green zones, bioclimatic studies and human comfort in the future development of urban planning. *Landsc Urban Plan* 2001;55:151–61.
- [69] Ghani S, Bialy EM, Bakochristou F, Gamaledin SMA, Rashwan MM, Hughes B. Thermal comfort investigation of an outdoor air-conditioned area in a hot and arid environment. *Sci Technol Built Environ* 2017;23:1113–31. <https://doi.org/10.1080/23744731.2016.1267490>.
- [70] LabVIEW. LabVIEW PID and fuzzy logic toolkit user Manual_FUZZYchapters, LabVIEW PID Fuzzy Log. Toolkit user man; 2009. p. 1–76.
- [71] WHO. Health factors involved in working under conditions of heat stress, Tech. Rep. 412; 1969.
- [72] Dominguez SA, De La Flor FJS. The effect of evaporative techniques on reducing urban heat, Santamouris, M., Kolokotsa, D. *Urban Clim. Mitig. Tech.* Routledge, London; 2016.
- [73] EuroWEATHER climate average, n.d. http://www.eurometeo.com/english/city/clima_select.
- [74] Joshi S, Gomekar S, Pokle S. Design of solar powered mist cooling system for a typical semi-outdoor area in Nagpur; 2016.
- [75] ENF solar, Solar panel global database, n.d. <https://it.enfsolar.com/pv/panel>.
- [76] Keirstead J, Sivakumar A. Using activity-based modeling to simulate urban resource demands at high spatial and temporal resolutions. *J Ind Ecol* 2012;16:889–900. <https://doi.org/10.1111/j.1530-9290.2012.00486.x>.